Chapter 5

Defects in Quasicrystals

J. BOHSUNG and H.-R. TREBIN

Institut für Theoretische und Angewandte Physik der Universität Stuttgart
Stuttgart
Federal Republic of Germany

Contents

APERIODICITY AND ORDER 2
Introduction to the
Mathematics of Quasicrystals

ISBN 0-12-040602-0

1 Introduction

As a rule, order is accompanied or even reveals itself by defects. Penrose patterns carry long-range translational and orientational order. Therefore one expects also typical structural defects to exist. In the search for defects of quasiperiodic systems it is helpful first to remember their periodic counterparts.

The classical structural defects in periodic crystals are dislocations, disclinations, dispirations, stacking faults, and twin boundaries (Nabarro, 1979; Friedel, 1981; Harris, 1970). Of these, dislocations may be found in any system of periodic translational symmetry, like the pattern of the fingerprints or the coat of zebras. The points, where dislocations pierce the surface of a crystal, can be made visible by etching techniques. Dislocations mediate plastic flow, catalyze crystal growth, and strongly influence all transport processes, in particular electric resistance. In two-dimensional hexagonal crystals, bound pairs of dislocations and anti-dislocations are present at any finite temperature and destroy the long-range translational order (Halperin and Nelson, 1978). Only quasi-long-range order of algebraically decaying Debye-Waller correlation functions can persist. At higher temperatures the pairs unbind and destroy the translational order, leaving, however, quasi-long-range bond-orientational order ("hexatic phase"; for most recent observation in liquid-crystal films, see Cheng *et al.*, 1987).

Disclinations in crystals perturb the alignment of lattice directions. Since disclinations carry a very high strain energy, they are seen in extremely soft crystals only, like the flux-line lattices of superconductors (Träuble and Essmann, 1968). It has been an important insight, that a disclination-antidisclination pair ("dipole") is equivalent to a dislocation. When these dipoles, abundant in the hexatic phase, are freed at high temperatures to isolated disclinations, the bond-orientational symmetry also breaks down, and the two-dimensional crystal becomes fluid.

In the tetrahedrally close-packed (Frank–Kasper) phases of metallic alloys, where most atoms gather to clusters in the form of icosahedra, there are lines, along which the icosahedra are widened by insertions of tetrahedral wedges (Shoemaker, 1988). The lines, which arrange into lattices of space-group symmetry, are interpreted as wedge-disclinations in a medium of bond-orientational order, which is a generalization of a nematic liquid crystal (Sadoc, 1983). Amorphous metals are viewed as irregular entanglement of disclination lines, whose crossing is inhibited by topological obstruction (Nelson, 1983; Widom, 1988).

Whereas dislocations are characterized by pure translational elements of the crystal space group—the Burgers vectors, and disclinations by rotational elements, the dispirations are associated with screw axes or mirror

glides, operations which appear only in nonsymmorphic space groups. Stacking faults are mismatches of crystal planes, frequently generated by splitting a dislocation into two of fractional Burgers vector and moving them apart. Finally, twin boundaries are interfaces between differently oriented crystals and are comprised of many dislocations. Icosahedral twinning of cubic crystallites is one controversial explanation of the non-crystallographic symmetries in material like shechtmanite (Shechtman *et al.*, 1984; Pauling, 1987).

There are several incentives to identify the analogues of dislocations and disclinations in quasicrystals. Penrose patterns are two-dimensional systems, and according to phase space counting fluctuations of the atomic displacements are so strong that exact long-range order is reduced to quasi-long-range order just as in periodic crystals (Levine *et al.*, 1985). What are the defects involved in the process? Are there purely translatory structural defects ("dislocations") and rotatory ("disclinations"), and are dipoles of the latter equivalent to the former? Is the motion of dislocations as simple (namely along glide planes) as in crystals, so that after unbinding of the dipoles these singularities move as free gas molecules? Does proliferation of dislocations in a quasi-periodic icosahedral phase induce the "icosahedratic" phase? Are disclinations the elementary excitations in pentagonal and icosahedral quasicrystals, which mediate the loss of long-range bond orientational order in transitions to the amorphous or fluid state?

On the way to an answer of these questions, we make use of the fact that the long range positional order of quasicrystals arises by projecting vertices of hypercubic lattices onto lower dimensional subspaces. The necessity of higher dimensions is motivated in Section 2 both in a continuum model and a microscopic model. In Section 3, dislocations and disclinations are constructed via the Volterra process in the hypercubic lattices. Suitable projection proves, that the singularities are not only accompanied by deformations in real space ("phonon strain"), but also by deformations in phase space ("phason strain"). In the microscopic model the phason strain manifests itself in the form of exceptional vertices, called mistakes (Lu and Birman, 1986). Thus disclinations and dislocations are accompanied by clouds of mistakes and become "dressed" like polarons. Also in Section 3 methods of algebraic topology are applied to the classification of singularities in quasiperiodic systems. It is ascertained that disclination dipoles are equivalent to single dislocations. Finally, dislocation motion is demonstrated by the example of a dislocation dipole, whose constituents slowly move apart.

Thus, the article is a contribution to the analysis of defects in quasicrystals and their kinetics. Before we treat the defected state, we remind of some properties of the perfect system.

2 The Perfect Quasicrystal

To construct quasicrystals, a variety of methods has been developed in the past. These can be divided into continuum approaches (see, for example, Kalugin *et al.*, 1985; Levin *et al.*, 1985; Jarić 1985; Bak, 1985; Troian and Mermin, 1985) and microscopic models (Penrose, 1974; de Bruijn, 1981; Kramer and Neri, 1984; Duneau and Katz, 1985; Katz and Duneau, 1986), both of which we are going to review briefly.

2.1 Some Aspects of Quasiperiodic Structures in the Density Wave Approach

Landau's theory of phase transitions answers the question, into which ordered phases an isotropic liquid (described by a constant mass density ρ_0) may condense below a critical temperature T_c (Landau and Lifshitz, 1980). During the condensation process the translational symmetry of the liquid phase is broken by an inhomogeneous mass density $\rho(\mathbf{r})$ which is superposed to ρ_0 and transforms like an irreducible representation of the symmetry group of the liquid phase.

These irreducible representations are labeled by wave vectors $\mathbf{K} \in R^d$ (d is the dimension of the space considered).

$$\rho(\mathbf{r}) = \sum_{\mathbf{K} \in R^d} \rho_{\mathbf{K}} e^{i\mathbf{K}\cdot\mathbf{r}} + cc. \tag{1}$$

The Landau free energy of the ordered phase is expanded into powers of $\rho_{\mathbf{K}}$:

$$F(P, T, \rho_{\mathbf{K}}) = F_0 + \tfrac{1}{2} \sum_{\mathbf{K}} A|\rho_{\mathbf{K}}|^2 + B \sum_{\mathbf{K}_1 + \mathbf{K}_2 + \mathbf{K}_3 = 0} \rho_{\mathbf{K}_1}\rho_{\mathbf{K}_2}\rho_{\mathbf{K}_3} + C \sum_{\mathbf{K}_1 + \cdots + \mathbf{K}_4 = 0} \rho_{\mathbf{K}_1}\rho_{\mathbf{K}_2}\rho_{\mathbf{K}_3}\rho_{\mathbf{K}_4} + \cdots \tag{2}$$

In the minimization process of F, the coefficients $A, B, C, \ldots$ pick out special wave vectors: A selects a shell $\mathbf{K} = \text{const}$, $B, C, \ldots$ select discrete sets of elements out of this shell. The choice of $B, C, \ldots$ fixes the stable structures.

2.1.1 Two-Dimensional Pentagonal Structures. If the fifth-order term dominates the expansion (2), in two dimensions the ground state mass density $\rho(\mathbf{r})$ is composed of five plane waves, whose wave vectors form an equilateral pentagon:

$$\rho(\mathbf{r}) = \sum_{i=1}^{5} \rho_{\mathbf{K}_i} e^{i\mathbf{K}_i\cdot\mathbf{r}} + \cdots \tag{3}$$

where $\sum_{i=1}^{5} \mathbf{K}_i = \mathbf{0}$ and the ellipses denote higher harmonics (see for example Bak, 1985). The density $\rho(\mathbf{r})$ is nonperiodic but nonetheless ordered.

To unveil the symmetry of this structure, one maps the five two-dimensional wave vectors $\mathbf{K}_i$ onto orthogonal vectors $\mathbf{K}_i^{(5)}$ of a five-dimensional space R^5 and formally establishes a five-dimensional density (Bak, 1985; Sachdev and Nelson, 1985):

$$\rho^{(5)}(\mathbf{x}) = \sum_{i=1}^{5} \rho_{\mathbf{K}_i} e^{i\mathbf{K}_i^{(5)} \cdot \mathbf{x}}, \qquad \mathbf{x} \in R^5. \tag{4}$$

This density represents a simple cubic structure in R^5.

We can reproduce $\rho(\mathbf{r})$, if we restrict $\rho^{(5)}(\mathbf{x})$ to a special plane P, spanned by two orthonormal vectors $\mathbf{z}_1, \mathbf{z}_2 \in R^5$:

$$\rho^{(5)}(\mathbf{x} \in P) = \sum_{i=1}^{5} \rho_{\mathbf{K}_i} e^{i\{\xi_1(\mathbf{K}_i^{(5)} \cdot \mathbf{z}_1) + \xi_2(\mathbf{K}_i^{(5)} \cdot \mathbf{z}_2)\}}. \tag{5}$$

Equation (5) is equivalent to Eq. (3), if we choose ξ_1, ξ_2 as the components of $\mathbf{r} \in R^2$ and $\mathbf{K}_i^{(5)} \cdot \mathbf{z}_{1,2}$ as the components K_{i1}, K_{i2} of $\mathbf{K}_i$.

We are now interested in those translations of $\rho^{(5)}(\mathbf{x})$ in R^5 which leave the Landau free energy of the corresponding two-dimensional system invariant. For a shift of $\rho^{(5)}$ by a vector $\gamma \in R^5$ we obtain:

$$\tilde{\rho}^{(5)}(\mathbf{x}) = \rho^{(5)}(\mathbf{x} + \gamma) = \sum \rho_{\mathbf{K}_i} e^{i(\mathbf{K}_i^{(5)} \cdot \mathbf{x} + \mathbf{K}_i^{(5)} \cdot \gamma)}. \tag{6}$$

From Eq. (6) it is seen, that the phases ϕ_i of $\rho_{\mathbf{K}_i} = |\rho_{\mathbf{K}_i}| e^{i\phi_i}$ may be interpreted as translational degrees of freedom in R^5: if we choose the origin of R^5 such that $\rho_{\mathbf{K}_i}$ is real when $\gamma = \mathbf{0}$, then

$$\phi_i = \mathbf{K}_i \cdot \gamma. \tag{7}$$

Inserting the complex coefficients $\rho_{\mathbf{K}_i}$ into the free energy expansion (2) one observes, that F only depends on the sum

$$\Gamma = \sum_{i=1}^{5} \phi_i = \sum_{i=1}^{5} \mathbf{K}_i \cdot \gamma, \tag{8}$$

which is the component of γ along the diagonal $\Delta = \sum_{i=1}^{5} \mathbf{K}_i^{(5)}$ in R^5.

Hence, the free energy is invariant under all translations in the four-dimensional subspace R^4 orthogonal to the subspace Δ spanned by Δ. R^4 consists of two mutually orthogonal two-dimensional planes: the physical plane P, whose vectors $\mathbf{u}$ represent pure in-plane translations of $\rho(\mathbf{r})$, and the "phase" plane $P_\perp$, whose vectors $\mathbf{v}$ cause phase shifts of the density waves without influencing the energy of ρ.

Thus, R^5 divides into three orthogonal subspaces:

$$R^5 = P \oplus P_\perp \oplus \Delta. \tag{9}$$

The four translational degrees of freedom of P and $P_\perp$, if position dependent, correspond to four hydrodynamic modes $\mathbf{u}(\mathbf{r})$ and $\mathbf{v}(\mathbf{r})$.

The two "phonon-like" excitations $\mathbf{u}(\mathbf{r})$ are equivalent to the displacive modes of usual periodic structures. The additional excitations $\mathbf{v}(\mathbf{r})$ are the analog of the "phasons" in incommensurate crystals. These modes appear because four of the five wave vectors $\mathbf{K}_i$ are linearly independent in the field of rational numbers (see for example Kalugin *et al.*, 1985).

2.1.2 Three-Dimensional Icosahedral Structures. A mass density $\rho(\mathbf{r})$ of icosahedral symmetry requires six density waves of wave vectors pointing to the corners of an icosahedron. This structure becomes stable by contributions of the sixth- and tenth-order term in the free energy expansion (2) (Bak, 1985).

Because all six wave vectors are rationally linearly independent, the icosahedral structures carry six hydrodynamic modes. Each may be interpreted as a translation in a six-dimensional space. The three shifts in physical space cause phonon-modes, the three degrees of freedom in the orthogonal space correspond to phasons.

2.2 *An Example for a Microscopic Model: The Pentagonal Quasiperiodic Pattern*

For the construction of microscopic models of quasicrystals in arbitary dimensions the projection formalism is very popular (Duneau and Katz, 1985). To obtain two-dimensional pentagonal quasiperiodic patterns, we start from a five-dimensional hypercubic lattice L_γ in R^5, which is shifted by a vector $\gamma \in R^5$:

$$L_\gamma = Z^5 - \gamma. \tag{10}$$

In R^5 a two-dimensional tiling plane P is embedded in such a way, that it remains invariant under the group C_5 of all cyclic permutations of the five canonical basis vectors $\mathbf{e}_i$ $(i = 1, \ldots, 5)$ of R^5.

Aside from P, C_5 leaves two other subspaces of R^5 invariant:

- the one-dimensional space Δ spanned by $\Delta = \sum_{i=1}^{5} \mathbf{e}_i$,
- another two-dimensional space $P_\perp$.

P, $P_\perp$ and Δ are mutually orthogonal, i.e. R^5 falls into three C_5-invariant subspaces as in Eq. (9).

From the lattice L_γ we select a special set of points inside a strip S, which is cut out of L_γ by moving the five-dimensional unit cube W^5 along the tiling plane P:

$$S = \{\mathbf{x} \in R^5 | \mathbf{x} = \mathbf{x}_T + W^5; \quad \mathbf{x}_T \in P\}. \tag{11}$$

The tiling arises, if all those lattice points and two-faces, which belong to the five-dimensional hypercubes inside S, are projected onto P.

The choice of the shift vector γ affects the tiling in three ways:

- Variations of γ in P lead to pure translations of the lattice.
- Variations of γ in $P_\perp$ preserve the local isomorphism (LI-)class (Katz and Duneau, 1986) i.e. any finite section of one tiling is found in every other tiling of the same LI-class, however, without global congruence in general.
- Variations of γ within Δ result in tilings of different LI-classes. The special class, where γ is orthogonal to Δ, is named after R. Penrose.

Quasicrystals of one and the same LI-class have identical physical properties, in particular the same free energy and diffraction spectrum, because up to all scales they contain identical sections.

2.3 *Comparison of Continuum and Microscopic Model*

The pentagonal structures of the continuum model (Section 2.1.1) and the microscopic approach (Section 2.2) display remarkable similarities:

- Both structures hide the symmetry of a five-dimensional simple cubic lattice.
- The shift vector γ of the microscopic model corresponds to the phases in the density wave picture:
  The "phonon"-variable $\mathbf{u}$ is equivalent to the projection of γ onto P. The "phason"-variable $\mathbf{v}$ corresponds to the projection of γ onto $P_\perp$. The phase shifts associated with a variation of $\mathbf{v}$ in the density wave picture are analogous to special rearrangements of rhombuses in the microscopic picture, such that the LI-class remains unchanged.
- Shifts of γ in Δ lead to patterns of different LI-classes, in the continuum model they produce structures $\rho(\mathbf{r})$ of differing free energy.

3 Defects in Quasicrystals

3.1 *Introduction*

In this chapter we illuminate some features of topological defects in quasicrystals.

- Section 3.2 is devoted to topological point defects like dislocations or disclinations in two-dimensional quasicrystals. We remind of analogous defects in periodic crystals and generalize the well-known methods used for their construction.

- In Section 3.3 we define topological defects in the density wave picture and compare their features with those of the microscopic approach.
- In Section 3.4 we analyse topological defects in quasicrystals with the help of homotopy theory.
- Sections 3.5 and 3.6 are addressed to line singularities in icosahedral quasicrystals and to a speculative remark on configurations.

3.2 *Construction of Topological Defects*

3.2.1 Dislocations in Periodic Crystals. If the plastic deformation of a perfect periodic crystal were initiated by parallel displacement of two crystal planes, a force would be necessary of the order of the shear modulus μ. However, in experiment forces smaller by 10^{-4} already cause plastic flow (see, e.g., Friedel, 1967).

This fact is explained by the concept of dislocations. Due to their presence the two planes are sheared by a consecutive motion. To understand this process we discuss dislocations from a microscopic geometric point of view.

The simplest type is the edge dislocation. It arises if an extra half plane is inserted into the crystal lattice (Fig. 1). The defect itself is the line L (or the point L in the case of the two-dimensional example of Fig. 1) where the half plane terminates. In L the lattice is structurally changed whereas outside of L it is only distorted without loosing the topology of the perfect lattice.

The motion of an edge dislocation is demonstrated in Fig. 2. Only a slight replacement of atoms near the defect core is requested to displace the dislocation by one lattice constant (Fig. 2b). After the dislocation has traversed the crystal, it appears as if the two halfs of the crystal have been sheared rigidly (Fig. 2c).

A general construction method for dislocations is the Volterra process (Friedel, 1967). It can also be applied for other types of line defects (like disclinations, see below). The Volterra process consists of the following steps (see Fig. 3):

1. Cut the crystal along an arbitrary surface Σ which is bounded by a line L (Fig. 3a).
2. Separate the two arising lips Σ_1 and Σ_2 by a vector $\mathbf{b}$, the Burgers vector of the dislocation, which has to be a lattice vector (Fig. 3b).
3. Fill the space between Σ_1 and Σ_2 with perfect crystal matter or remove extra matter.
4. Glue the lips together. Because $\mathbf{b}$ is a lattice vector, this process restores the lattice everywhere outside the line L except for continuous deformations (Fig. 3c).

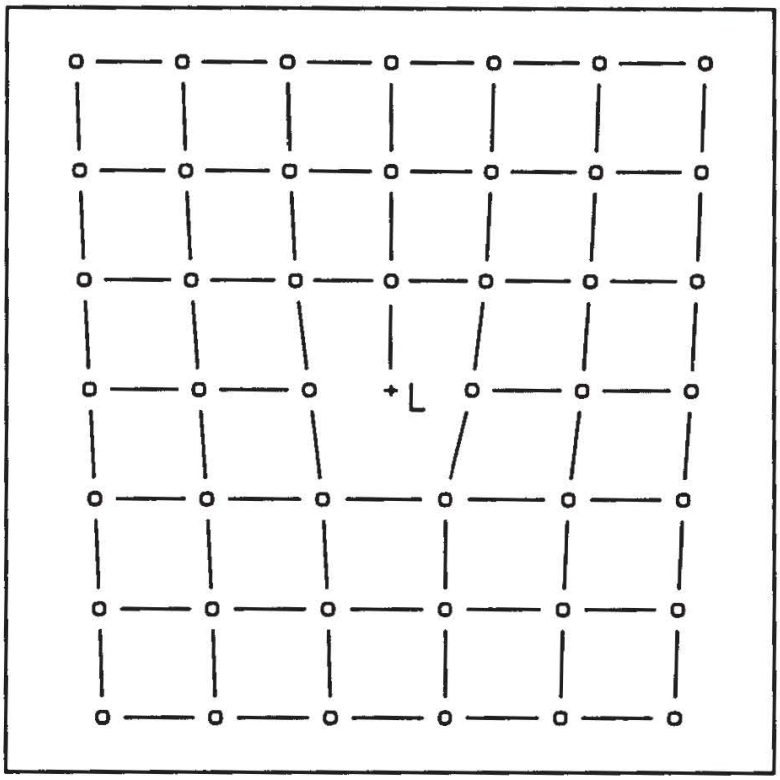

Figure 1. Edge dislocation in a square lattice. An additional row of atoms terminates in the defect core L. At L, the topology of the lattice is changed, outside L the lattice is only distorted.

From the description it becomes clear that the final result is independent of the special choice of Σ. The defect is completely defined by its position L and by the Burgers vector **b**. Only along L the lattice geometry is essentially disturbed, outside it is just distorted.

3.2.2 Creation of Dislocations in a Two-Dimensional Quasicrystal. In this section we construct a dislocation in a two-dimensional pentagonal

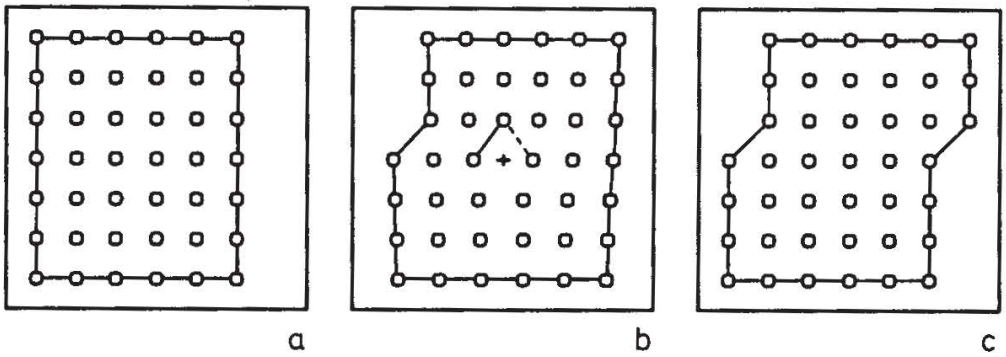

Figure 2. Motion of an edge dislocation. a. Initial state without dislocation. b. Propagating dislocation; only the atoms close to the core jump. c. Final state equivalent to a rigid shear. (The dislocation has traversed the whole crystal.)

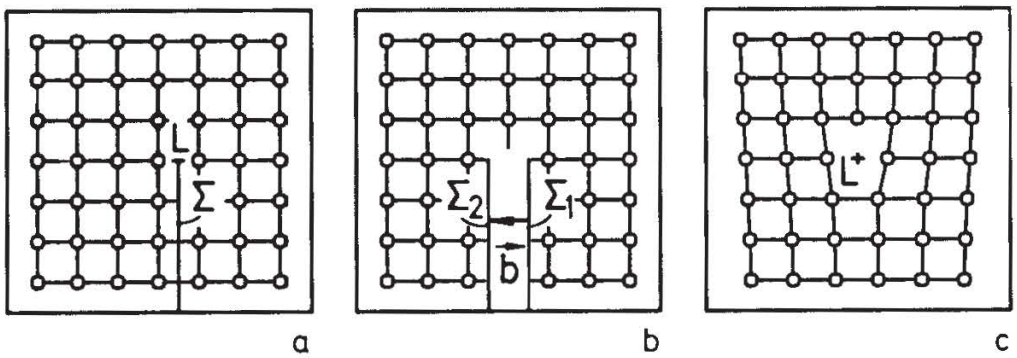

Figure 3. Volterra process for the construction of a dislocation in a square lattice (see text for detailed explanation).

quasicrystal (Bohsung and Trebin, 1987). We proceed as close as possible to the case of periodic crystals.

In the quasicrystalline pattern itself a Volterra process cannot be performed because translational symmetry is absent. We cannot specify any lattice vector linking two equivalent lips of a cut.

In analogy to the crystalline case one could remove a piece of one of the trails which wind through the pattern (see Fig. 4). Indeed the remaining lips match, but along the glue types of vertices originate which do not belong to the original LI-class (these vertices are marked in Fig. 4). The result is not a point singularity, but a linear stacking fault.

Although this attempt is in vain, it guides us in how to proceed, if we analyse the removal of a trail in terms of the five-dimensional hypercubic lattice L.

Every trail in the pattern corresponds uniquely to a four-dimensional canonical hyperplane of L (Gähler and Rhyner, 1985). Therefore, the removal of a trail is equivalent to the removal of a hyperplane in L, i.e. to a Volterra cut in the hypercubic lattice, which generates a dislocation. Only the transfer to the tiling plane is not correct.

To carry out this step properly we have to remember the strip S which is embedded in the hypercubic lattice L_γ with an irrational slope (see Section 2.2). Its presence destroys the original cubic symmetry of the lattice. Therefore, the two now four-dimensional lips Σ_1 and Σ_2 resulting from the Volterra cut are no longer equivalent.

For the following it proves useful to change from the "active" viewpoint of Section 2.2, where the strip is fixed in R^5 and the lattice is translated, to the equivalent "passive" one with fixed lattice L and shifted strip $S_\gamma = \gamma + S$.

Figure 5 illustrates the problem for a three-dimensional cubic lattice with an embedded strip S_γ. The two lips Σ_1 and Σ_2 cut out sections of the strip (they are hatched in Fig. 5). The sections do not touch, when the two lips are

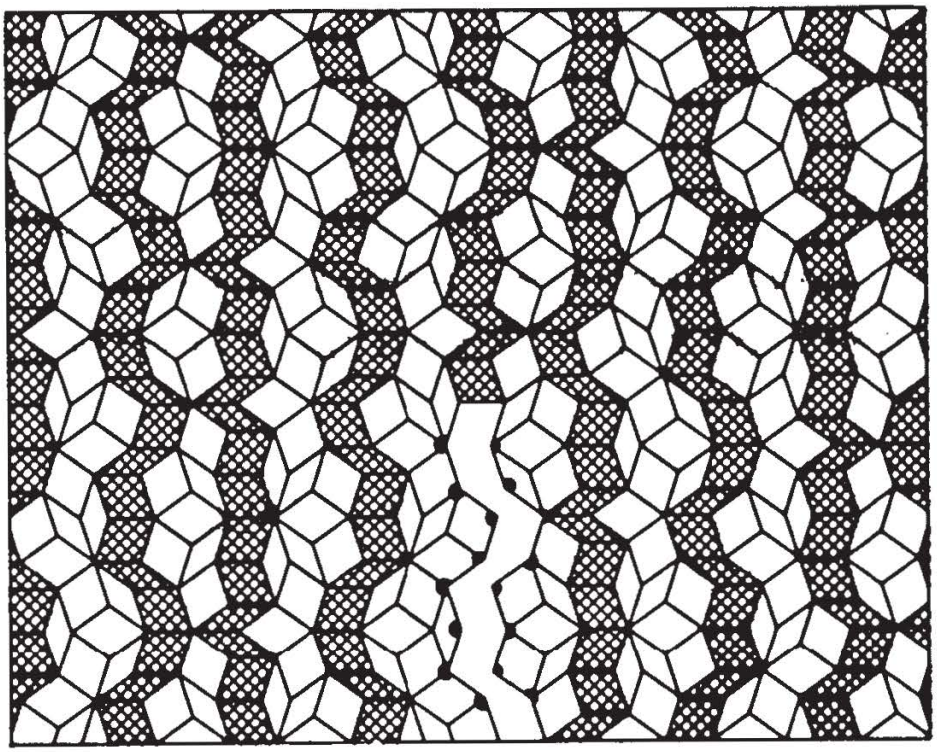

Figure 4. Quasicrystal of the Penrose-LI-class. Some of the trails, which run through the lattice, are hatched. Removing a piece of a trail and glueing the lips together leads to vertices outside the original LI-class (marked by dots).

matched. This is the reason for the appearance of a stacking fault in the pattern of Fig. 4.

How to solve this problem becomes clear in Fig. 6: if the strip which arrives at Σ_2 is bent around the singular line (in the five-dimensional case around the singular three-dimensional space respectively), the two sides of the strip match again. This bending is performed, if the shift vector γ is changed from an initial value γ_{start} at Σ_1 to a vector γ_{end} at Σ_2 and if γ_{end} differs from γ_{start} exactly by the Burgers vector $\mathbf{b}$:

$$\gamma_{\text{end}} = \gamma_{\text{start}} + \mathbf{b}. \tag{12}$$

In the case of our two-dimensional quasicrystal the Burgers vector $\mathbf{b}$ is a lattice vector $\mathbf{b} \in Z^5$.

To prove the necessity of relation (12), we choose the lip Σ_1 orthogonal to $\mathbf{e}_1$:

$$\Sigma_1 = \{\mathbf{x} \in R^5 \,|\, \mathbf{x} \cdot \mathbf{e}_1 = K_1; K_1 \in Z\}. \tag{13}$$

The second lip Σ_2 arises from the first by action of a translation $\{1, \mathbf{b}\}$[1] onto Σ_1:

$$\Sigma_2 = \{1, \mathbf{b}\}\Sigma_1 = \{\mathbf{x} \in R^5 \,|\, \mathbf{x} \cdot \mathbf{e}_1 = K_1 + \mathbf{b} \cdot \mathbf{e}_1; K_1 \in Z, \mathbf{b} \in Z^5\}. \tag{14}$$

[1] $\{1, \mathbf{b}\}$ is an element of the space group of the five-dimensional crystal lattice. $\mathbf{b}$ denotes the Burgers vector of the dislocation.

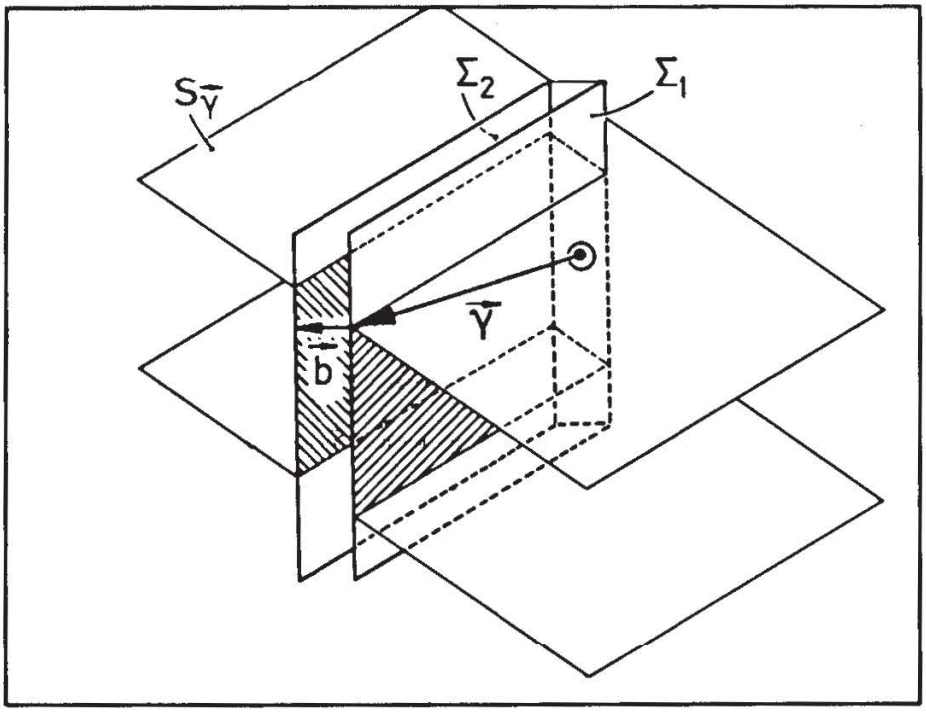

Figure 5. Schematic illustration of a Volterra cut in a three-dimensional cubic lattice with embedded strip S_γ. The two intersections (hatched) of the lips Σ_1 and Σ_2 with S_γ, respectively do not touch after glueing the lips together.

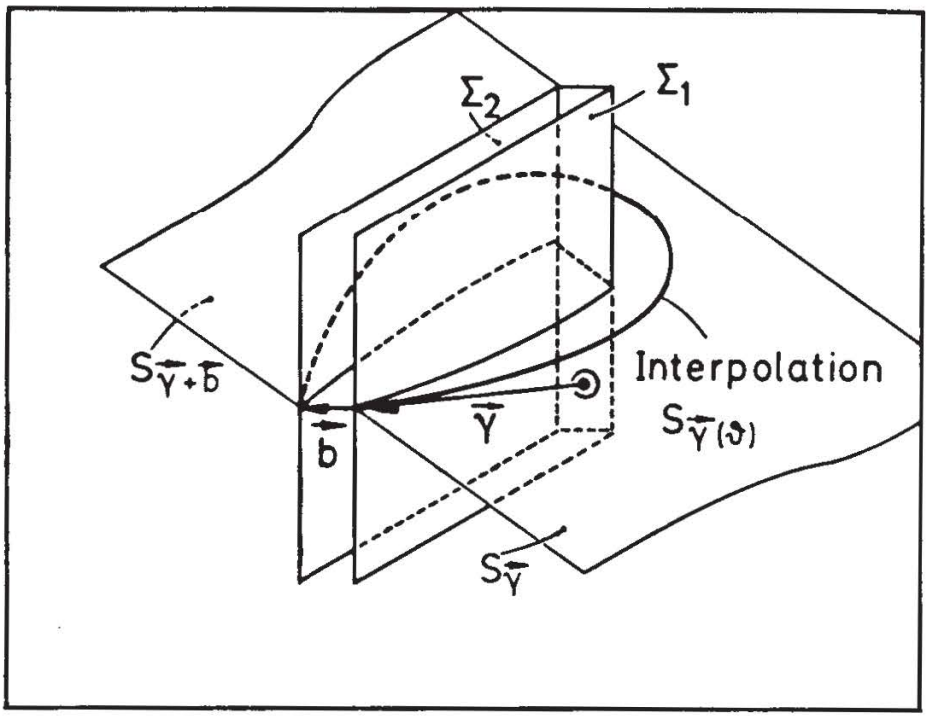

Figure 6. Interpolation between the strips S_γ and $S_{\gamma+b}$ (schematically). For clarity only the top of each strip is depicted.

Apart from the action of $\{1, \mathbf{b}\}$ on the lip Σ_1 we have to study the behaviour of the strip $S_{\gamma_{\text{start}}}$, if it is translated by $\mathbf{b}$ (compare with Eq. (11), the strip is now shifted by a vector γ):

$$S_{\gamma_{\text{end}}} = \{1, \mathbf{b}\} S_{\gamma_{\text{start}}} = \{\mathbf{x} \in R^5 \mid \mathbf{x} = \mathbf{x}_T + \gamma_{\text{start}} + \mathbf{b} + W^5; \mathbf{x}_T \in P\}. \quad (15)$$

The right hand side describes a strip with shift vector $\gamma_{\text{start}} + \mathbf{b}$.

To explicitly construct a dislocation in a two-dimensional quasicrystal, we have to choose an interpolation rule between γ_{start} and γ_{end}. For simplicity we interpolate linearly in the polar angle θ, as we encircle the core of the defect in the tiling plane:

$$\gamma(\theta) = \gamma_{\text{start}} + \frac{\theta}{2\pi} \mathbf{b}. \quad (16)$$

A dislocation with the same interpolation formula but in the frame of the method of Fibonacci grids has already been constructed by Socolar *et al.* (1986).

Our strip in R^5 is now bent due to the varying $\gamma(\theta)$. On the path around the singular point the pattern is composed of many pieces of tilings according to different shift vectors $\gamma(\theta)$. In the selection of these pieces there is still some arbitrariness due to the interpolation and the shift vectors γ involved.

Which pieces are suitable is decided from energetics. We demand all local structures to be energetically degenerate. Why, is explained by a look on a normal cubic crystal with dislocation: the local structure outside the core of the defect is everywhere cubic. In periodic crystals, the environment of the dislocation belongs to *one structure* (for instance a cubic one). The generalization to quasicrystals consists in taking *all the pieces from the same LI-class*. From Section 2.1 we know, that the LI-class is specified by the projection of γ onto Δ (i.e. by $\gamma \cdot \Delta$). So we have to restrict the shift vector $\gamma(\theta)$ in Eq. (16) by the condition:

$$\gamma(\theta) \cdot \Delta = \text{const.} \quad (17)$$

From Eq. (16) we recognize, that Eq. (17) allows only Burgers vectors orthogonal to Δ:

$$\mathbf{b} \cdot \Delta = 0. \quad (18)$$

In Fig. 7a dislocation in a Penrose pattern (i.e. $\gamma \cdot \Delta = 0$, see Sect. 2.1) of Burgers vector $\mathbf{b} = (-1, 1, 0, 0, 0)$ is presented.

Figure 7a shows the defect before the lips of the four-dimensional hyperplanes have been glued together. Two trails in the pattern are removed according to the two nonzero components of $\mathbf{b}$.

In Fig. 7b the lips are linked, they match perfectly.

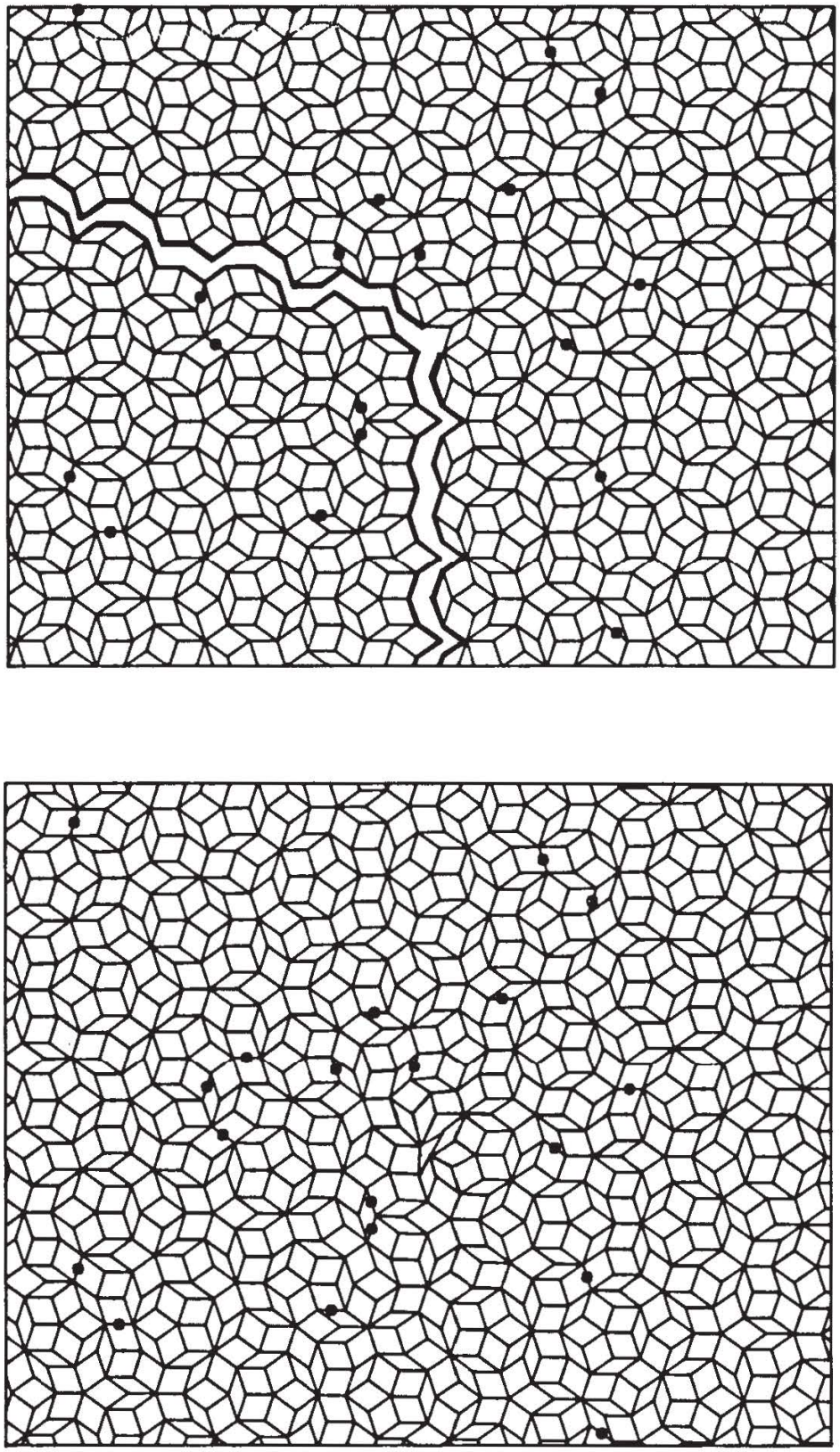

Figure 7. Dislocation in a Penrose pattern with Burgers vector $\mathbf{b} = (-1, 1, 0, 0, 0)$. The dots mark those edges which are bounded by vertices outside the Penrose-LI-class. a. Undistorted state. Two trails are removed according to the two nonzero components of **b**. b. Final state after glueing the lips together.

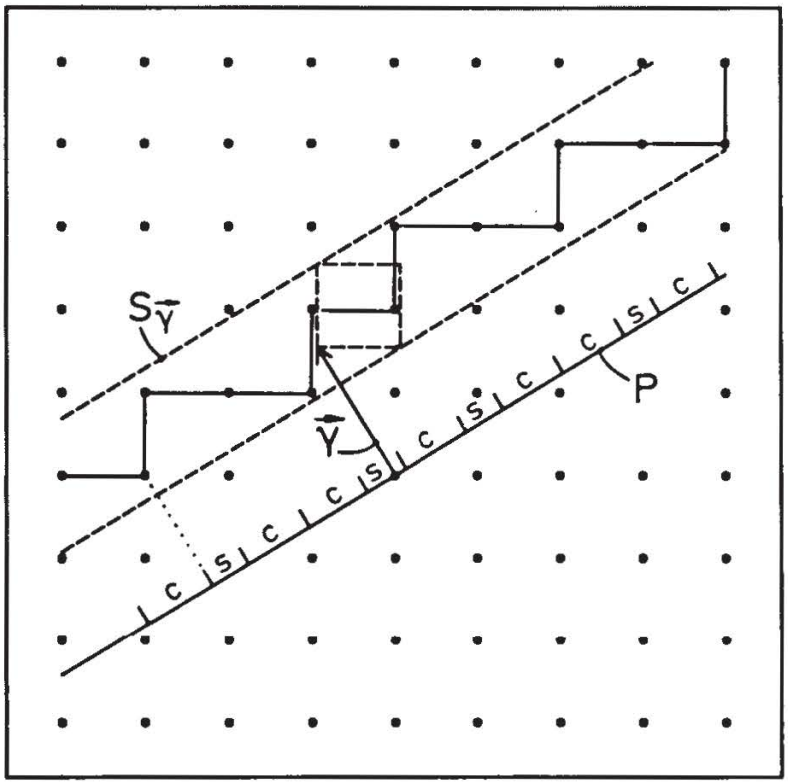

Figure 8. Construction of a one-dimensional quasicrystal by the projection method.

3.2.3 Mistakes. Looking carefully on the defected pattern of Fig. 7 one notices some vertices outside the chosen LI-class, although restriction (17) is valid. In the following we call these exceptional vertices mistakes. Mistakes turn out to be really new and interesting aspects of defects in quasicrystals compared to those in periodic crystals. In this section we illustrate mistakes in a one-dimensional quasicrystal and discuss some of their geometrical properties in two-dimensional quasiperiodic patterns. A deeper understanding of mistakes is gained in Section 3.3 where defects in the microscopic picture are compared with those in the continuum model.

The decisive difference in the construction process of defects in quasicrystals is the bending of the strip, as is demonstrated for the case of a one-dimensional quasicrystal in Fig. 8: a tiling line P is embedded in a square lattice with irrational slope. The lattice points and all one-dimensional faces of the squares inside the strip S_γ are projected onto the tiling line, leading to a sequence of long (c) and short (s) distances. The LI-class depends only on the slope of P and not on the choice of the shift vector γ (Katz and Duneau, 1986).

In Fig. 9 the strip interpolates between S_γ and $S_{\gamma+\varepsilon}$. The tiling line itself pertains its constant slope through the lattice, i.e. the LI-class does not change along it.

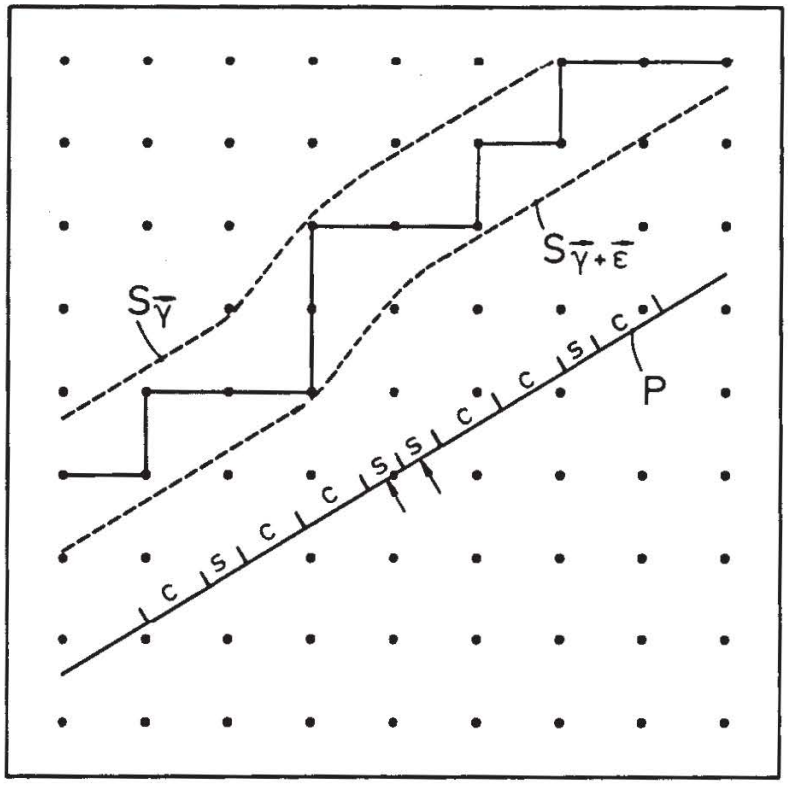

Figure 9. Interpolation between two one-dimensional quasicrystals of different shift vectors. In the transition region two short segments are adjacent (labeled by arrows), a sequence which is not allowed in a perfect quasicrystal of this LI-class.

Where the strip is curved, some sequences occur, which do not belong to the LI-class of the perfect system, for example the two neighbouring short segments in Fig. 9.

We now understand mistakes as points in the pattern, where different locally perfect tilings of one LI-class do not fit. In crystals, all local structures are identical and, therefore, match perfectly.

Mistakes in two-dimensional quasicrystals display another interesting property, which becomes visible, if we mark the trails in the pattern and their boundary lines. The trails jump at a mistake as seen in Fig. 10. These jumps remind of phase shifts and of the phasons occurring in the continuum model (Section 2.1). We discuss this relation in Section 3.3.

3.2.4 Disclinations in Periodic Crystals. A disclination also is constructed by a Volterra process. Now, however, the two lips are related by a lattice rotation instead of a translation. In Fig. 11 a 90°-disclination is shown in a square lattice. Figure 11a presents the undistorted lattice; in Fig. 11b the lips are closed.

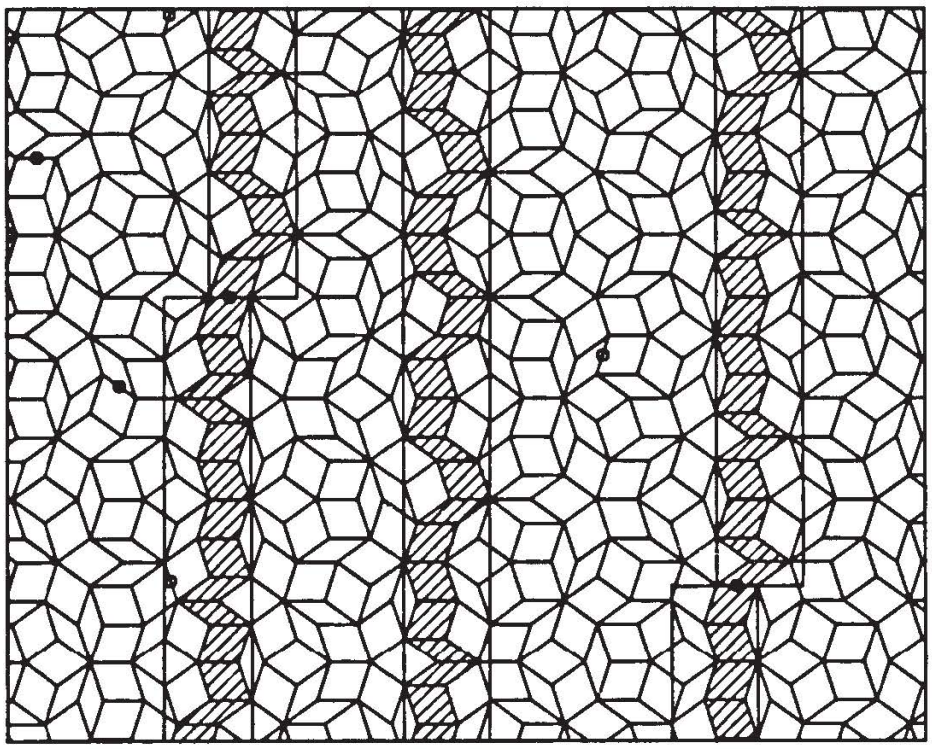

Figure 10. Mistakes cause phase shifts of trails.

3.2.5 Construction of a Disclination in a Two-Dimensional Quasicrystal. As in the case of the dislocation it is generally not possible to construct a disclination by cutting out or adding a sector of the tiling, because there is no global fivefold symmetry (an exception is the highly singular pattern of zero shift vector). Therefore, we again carry out the Volterra process in the five-dimensional hypercubic lattice and bend the strip in a suitable manner.

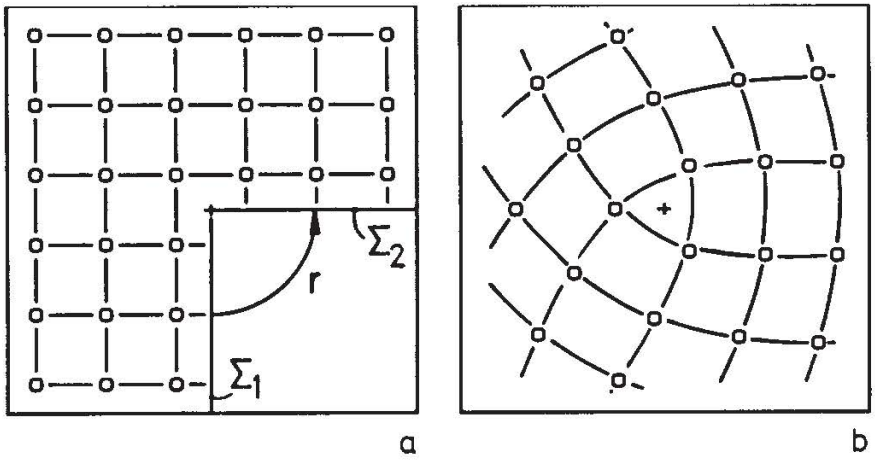

Figure 11. Volterra process for the construction of a 90°-disclination in a square lattice. a. A 90°-sector is removed from the lattice. Lips Σ_1 and Σ_2 are equivalent. b. Final state after glueing the lips together.

In the process we have to choose a group of rotations which map the two lips Σ_1 and Σ_2 onto each other. It seems to be obvious to take all rotations of the full point group[2] of the hypercubic lattice. But as before we have to take care that the resulting pattern contains only local tilings of one LI-class.

The rotations, which leave the LI-class invariant are discussed in Section 3.4, where the defects are classified by topological tools. They are the cyclic permutations of the canonical basis vectors in R^5 yielding the group C_5. This restricted set does not change the orientation between P and Z^5, when the two lips are closed and the lattice is distorted[3].

To transfer the disclination from the hypercubic lattice to the pattern, it is again necessary to bend the strip, so that the intersections of Σ_1 and Σ_2 with the strip match after glueing.

Figure 12 demonstrates how to proceed for a 90°-disclination in a three-dimensional lattice with irrationally embedded strip S_γ.

The two lips match, if the strip at Σ_2 corresponds to a shift vector γ_{end} which is rotated by 90° with respect to γ_{start}.

Hence, to create a disclination in a pentagonal quasicrystal, the shift vector γ_{start} has to be rotated by an element of C_5.

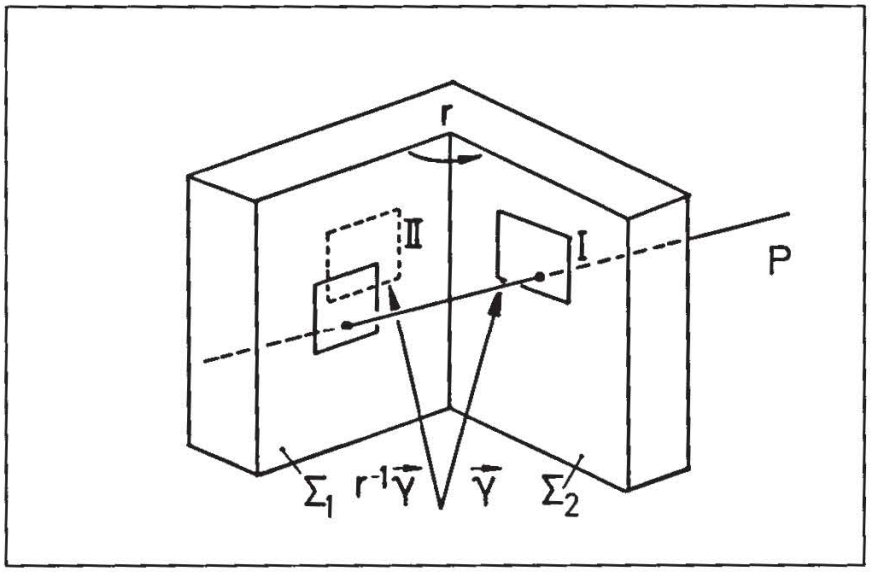

Figure 12. Schematic illustration of a disclination in a cubic lattice with embedded strip S_γ. For clarity the strip itself is not shown, only its intersections with the two lips Σ_1 and Σ_2. Intersection I of the strip S_γ with Σ_1 matches perfectly with intersection II of $S_{r^{-1}\gamma}$ with Σ_2, when the sector is closed.

[2] This group is the hyperoctahedral group $\Omega(5)$ (Kramer and Neri, 1984).

[3] This orientation determines the LI-class of the tiling. If it is changed, even the shapes of the rhombs alter.

For a proof of this statement, choose Σ_1 orthogonal to $\mathbf{e}_1$:

$$\Sigma_1 = \{\mathbf{x} \in R^5 \mid \mathbf{x} \cdot \mathbf{e}_1 = K_1; K_1 \in Z\}. \tag{19}$$

Σ_2 arises from Σ_1 by a rotation $\{r, \mathbf{0}\}$, where $r \in C_5$:

$$\Sigma_2 = \{r, \mathbf{0}\}\Sigma_1 = \{\mathbf{x} \in R^5 \mid (r^{-1}\mathbf{x}) \cdot \mathbf{e}_1 = K_1; K_1 \in Z\}. \tag{20}$$

The element $\{r, \mathbf{0}\}$ acts on the strip $S_{\gamma_{\text{start}}}$ as follows (cp. Eq. 11):

$$\{r,\mathbf{0}\}S_{\gamma_{\text{start}}} = \{\mathbf{x} \in R^5 \mid \mathbf{x} = (r^{-1}\mathbf{x}_T) + (r^{-1}\gamma_{\text{start}}) + W^5; \mathbf{x}_T \in P\}. \tag{21}$$

$r^{-1}\mathbf{x}_T$ is again a vector of P.

The right hand side of Eq. (21) describes a strip with a shift vector $\gamma_{\text{end}} = r^{-1}\gamma_{\text{start}}$.

In Fig. 13, an example for a 72°-disclination in a Penrose pattern is depicted, where we have chosen the following interpolation formula between γ_{start} and γ_{end}:

$$\gamma_i(\theta) = \gamma_{\text{start},i} + \frac{\theta}{8\pi/5} \cdot \{\gamma_{\text{start},i-1} - \gamma_{\text{start},i}\}; \; i = 1, \ldots, 5 \tag{22}$$

γ_i is the i-th component of γ, θ is again the polar angle of the tiling plane. Note, that the strip is bent before the lips are glued together, so $0 \leqslant \theta < 8\pi/5$.

Figure 13a shows the disclination with open sector, in Fig. 13b the sector is closed. As in the case of dislocated quasicrystals, mistakes accompany the singularity.

3.2.6 Dislocations as Disclination Dipoles. The topological classification of defects (see Section 3.4) proves that dislocations of Burgers vector $\mathbf{b}$ correspond to disclination dipoles.

In Fig. 14 this fact is illustrated for a dislocation in a quadratic lattice with Burgers vector $\mathbf{b} = (-2, -2)$. D can be considered as the center of a 90°-disclination (compare with Fig. 11). Point A (the three points have to be identified) marks an antidisclination, i.e. a disclination where a sector of extra matter is added.

Figure 15 presents the analogous case for a dislocation of Burgers vector $\mathbf{b} = (0, -2, 2, 2, -2)$ in a two-dimensional quasicrystal. As in the crystalline case we can identify the two cores D and A of a disclination dipole. For a more detailed investigation see Section 3.4.5.

3.3 Defects in the Continuum Approach

Frequently, it is sufficient to describe the physical properties of topological defects in crystals phenomenologically in terms of elasticity theory.

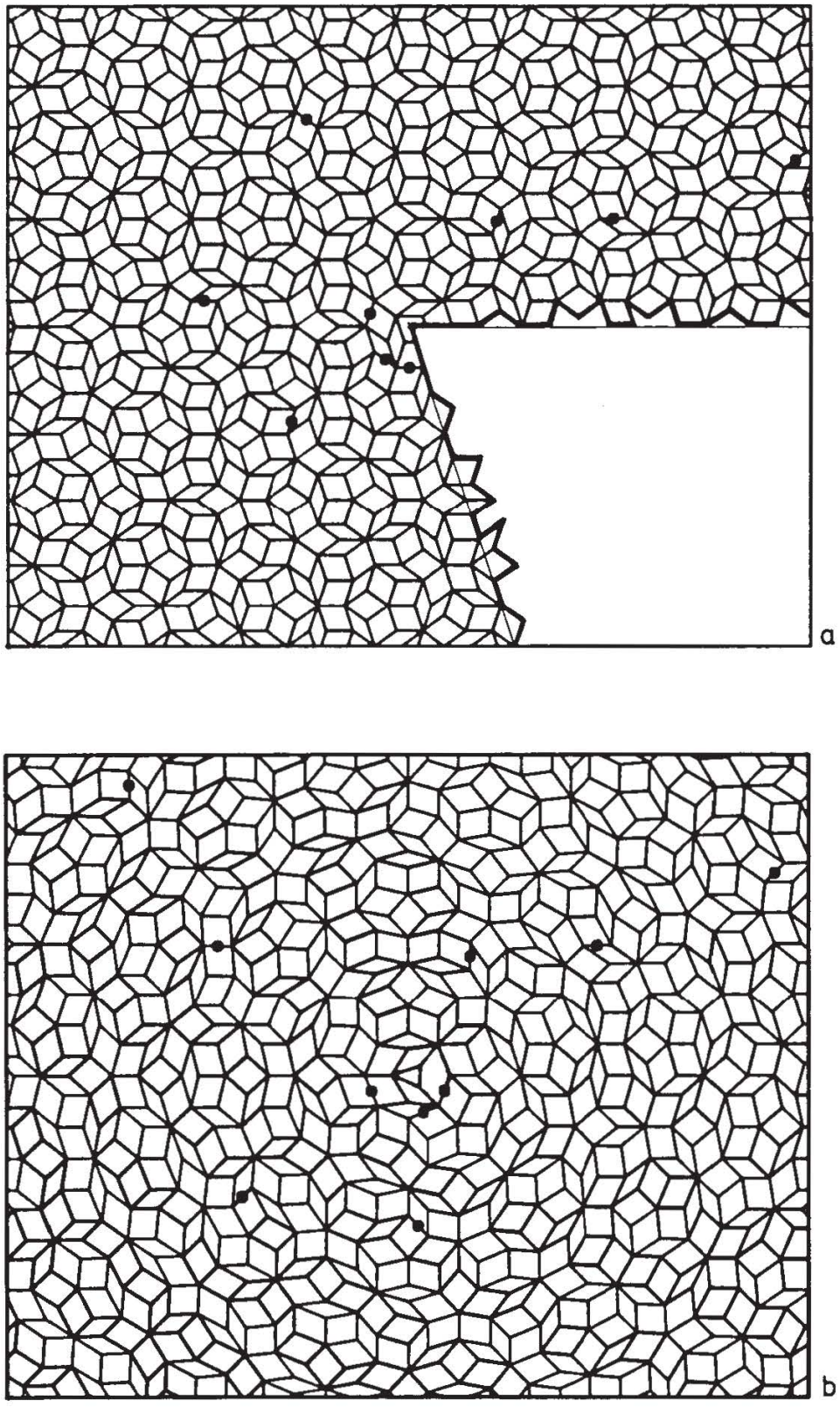

Figure 13. 72°-disclination in a Penrose pattern. As in the case of dislocations, several mistakes are present. a. Undistorted state. The lips match. b. Final state, when the sector is closed.

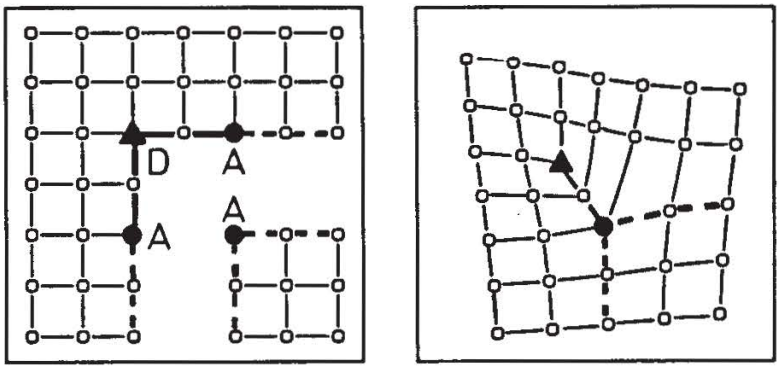

Figure 14. A dislocation of Burgers vector $\mathbf{b} = (-2, -2)$ in a square lattice is equivalent to a disclination dipole. a. Undistorted state. D labels the disclination, the three points A, which have to be identified, mark the antidisclination. b. Final state. Instead of the normal coordination number 4 the disclination is only threefold coordinated whereas the antidisclination has five bonds.

To define a dislocation in this framework, we consider a closed loop C which encircles the dislocation core L. To every point $\mathbf{r}$ of C we ascertain a vector $\mathbf{u}(\mathbf{r})$ describing the displacement relative to the perfect state.

If we sum up all displacements $\mathbf{u}$ on C, the result will not be zero but a Bravais lattice vector of the crystal, denoted Burgers vector (Friedel, 1967):

$$\oint d\mathbf{u} = \oint_C \frac{\partial \mathbf{u}}{\partial s} ds = \mathbf{b} \tag{23}$$

For a disclination the net displacement is given by:

$$\oint d\mathbf{u} = 2 \sin \frac{\Omega}{2} \boldsymbol{\omega} \times \mathbf{r}. \tag{24}$$

Ω is the angle between the two lips Σ_1 and Σ_2, and $\boldsymbol{\omega}$ is the rotation axis. Equations (23) and (24) demonstrate, that the displacement field of a crystal with topological defect is not integrable, i.e. the space is no longer simply connected.

To arrive at all aspects of a topological point defect in a pentagonal quasicrystal, we have to study the corresponding defect in the five-dimensional hypercubic structure $\rho^{(5)}(\mathbf{x})$ (Section 2.1.1). In analogy to the crystalline case the displacement $\gamma(\mathbf{x})$ of every point $\mathbf{x} \in R^5$ is measured relatively to its position in the perfect state on a closed loop around the defect core. As in the microscopic picture (Section 3.2.2) we restrict γ to vectors of $P \oplus P_\perp$.

A dislocation in the density $\rho^{(5)}(\mathbf{x})$ carries a Burgers vector

$$\oint d(\mathbf{u} + \mathbf{v}) = \mathbf{b} \in Z^5. \tag{25}$$

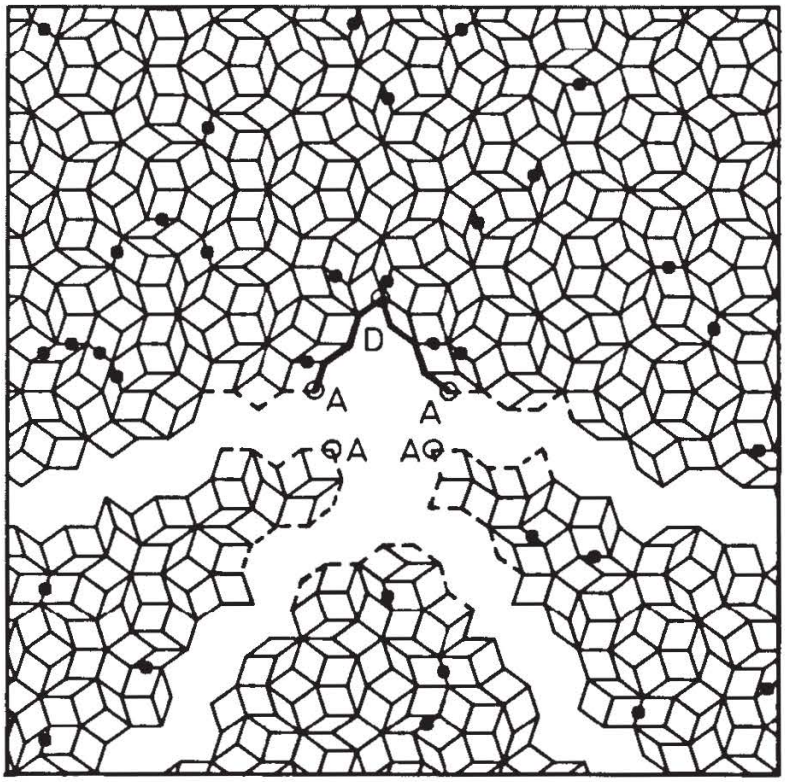

Figure 15. Equivalence between a dislocation of Burgers vector $\mathbf{b} = (0, -2, 2, 2, -2)$ and a 72°-dislocation dipole. The two cores are marked by A (antidisclination, the four points have to be identified) and D (disclination).

Any Burgers vector must have a component in $P_\perp$ due to the irrational slope of P in Z^5 (Levine *et al.*, 1985).

In the strain field about the defect, therefore, both fields $\mathbf{u}(\mathbf{x})$ and $\mathbf{v}(\mathbf{x})$ must participate. Thus every dislocation (and also every disclination) in a quasicrystal is accompanied by a phason strain $\mathbf{v}(\mathbf{r})$ in addition to the usual phonon strain $\mathbf{u}(\mathbf{r})$.

The dynamics of quasicrystals in the density wave model have been described in a hydrodynamic theory of Lubensky *et al.* (1985). Whereas the "in-plane" displacements $\mathbf{u}(\mathbf{r})$ are associated with normal sound modes, the modes coupled with $\mathbf{v}(\mathbf{r})$ are not propagating but rather diffusive.

As analysed by Lubensky *et al.*, (1986), the diffusive character of the phasons which follow dislocations reduces their mobility by up to four orders of magnitude and hence may greatly influence the plastic properties of quasicrystals.

In the microscopic picture, the phason strain is expressed by the occurence of mistakes (see also Socolar *et al.*, 1986). The motion of a dislocation is accompanied by mistakes moving through the quasicrystal by local rearrangements of vertices. In Section 4 the motion of a dislocation dipole and its accompanying mistakes is studied in detail.

3.4 *The Topological Classification of Defects in Quasicrystals*

Methods of algebraic topology have been developed in the last decade to classify defects in ordered media (for a review, see for example Mermin (1979) and Trebin (1982)). In this section, we are going to apply these methods to defects in quasicrystals.

3.4.1 Introductory Remarks. The basic concepts of the topological defect classification are introduced via a simple example, the isotropic planar ferromagnet. At high temperatures, the elementary ferromagnets are disordered; there is no macroscopic magnetization. Below the Curie temperature, the magnets start to align, and the arising order is characterized by a two-dimensional magnetization vector $\mathbf{m}$, which one may draw from the origin of an order parameter space $X = R^2$. The length of $\mathbf{m}$ is determined by temperature, the direction of $\mathbf{m}$, however, by chance (unless an orienting field is present). Also possible would be a magnetization $\tilde{\mathbf{m}}$ of different direction, but identical magnitude. The heads of all allowed magnetization vectors cover a circle S^1, which is denoted reduced order parameter space V. In practice the macroscopic magnetization varies in space due to growth conditions, boundary conditions, or external fields. The system is described by a mapping $R^d \to X$ from d-dimensional physical space (here $d = 2$) into order parameter space. In case of weak variations, the length of the vectors remains constant. The field is then valued not in the full order parameter space X, but only in the reduced one, V. Singularities, or defects, are now points, lines, or walls, where the reduced order parameter is not defined, as in the two examples of Fig. 16. Defects are denoted topologically

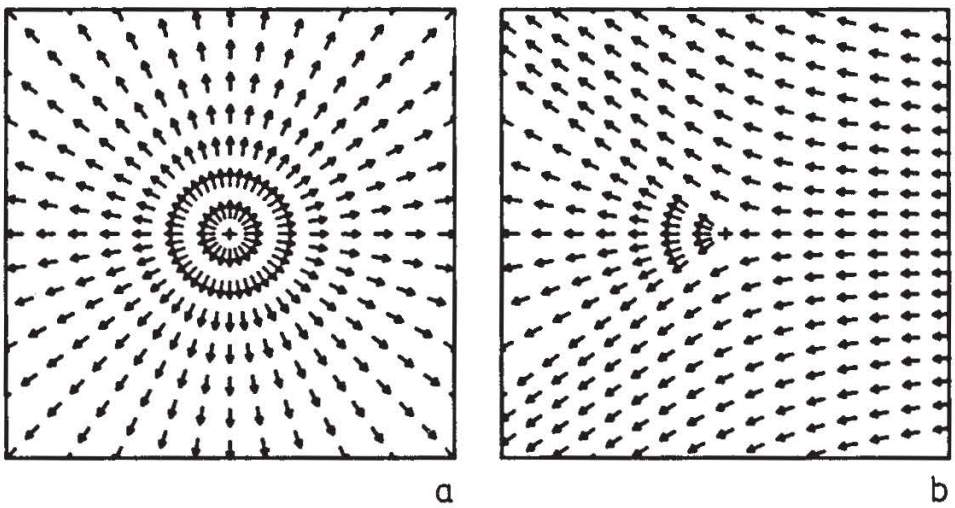

Figure 16. Point defects in a two-dimensional isotropic ferromagnet. a. Topologically stable point defect. b. Topologically unstable point defect.

stable, if they cannot be smoothed out by a change of the field in a small neighborhood of the singular set. Removal of the topologically stable source singularity of Fig. 16a, for example, requires a global rearrangement of the field, which (in an infinite system) costs an infinite amount of energy. The topologically unstable singularity of Fig. 16b can vanish by just local surgery.

In general, there are many types of topologically stable defects, like sinks, sources, crosspoints, or circulations for the planar ferromagnet. To distinguish them and to place them into classes, one can use the following equivalence relation, known as "Kléman–Toulouse" principle (Toulouse and Kléman, 1976): two singularities are equivalent or belong to the same class, if the core of one can be replaced by the core of the other. The locally restricted exchange of cores allows the transformation of one defect into the other by a small amount of energy, whereas for nonequivalent defects the transformation into another type requires an energetically costly global modification of the field. With the Kléman–Toulouse-principle the defect classification has become a problem of how to extend a continuous field over neighbourhoods of singularities, which can be attacked by topological tools.

In case of the planar ferromagnet each point singularity is labelled by an integer—the winding number, which is found in the following way: one encircles the defect along a closed path and draws the vectors, which one meets, from a common origin in order parameter space. This procedure yields a closed loop in the reduced order parameter space $V = S^1$, and the number of times, which the loop winds around the circle S^1, is the label of the singularity. Loops of winding number zero classify the topologically unstable defects. If two defects merge, their winding numbers add. In general, point singularities in the plane and line singularities in three-space are tested by closed contours (these are known as Burgers circuits in crystals). The values of the reduced order parameter along the contour form a loop in V, whose homotopy class (consisting of the loop and all those into which it is continuously deformable) labels the defect. The set of homotopy classes has the structure of the conjugacy classes of a group—the fundamental group $\pi_1(V)$ of the reduced order parameter space V, which expresses connectivity properties of V. If $\pi_1(V)$ is abelian, each conjugacy class contains only a single group element, which directly labels the defect. The unit element corresponds to the unstable singularities, defect merger to the product of group elements or conjugacy classes. In the present example, the fundamental group $\pi_1(V = S^1)$ is the (abelian) group of integers, and its elements correspond to the winding numbers.

Point singularities in the three-space are tested by two-spheres S^2. The reduced order parameters on this sphere form a sphere in V. The singularities

are labelled by the homotopy classes of spheres in V. These again have—in essence—the structure of a group, denoted second homotopy group $\pi_2(V)$. Walls in three space are tested by the zero-sphere S^0, which consists of two points. The labelling set, $\pi_0(V)$, corresponds to the different connected components of V.

The crucial step on the way to the defect classification is to determine the reduced order parameter space V. Frequently a group G is acting transitively on V, which says, that it can transform any element $v \in V$ into any other. In the case of a three-dimensional isotropic ferromagnet, where the reduced order parameter is a three-dimensional vector of fixed length, and $V = S^2$ the two-sphere, this is the group $SO(3)$ of all rotations. Let us choose a representative point in S^2, say the vector $\mathbf{m}_0$ along the z-direction, and another point $\mathbf{m}$, that is obtained from $\mathbf{m}_0$ via a rotation $g \in SO(3)$: $\mathbf{m} = g\mathbf{m}_0$. The set of all rotations turning $\mathbf{m}_0$ into $\mathbf{m}$ is the left coset gH, where H is the symmetry group of $\mathbf{m}_0$, consisting of the rotations about the z-axis: $H = SO(2)$. The points in $SO(3)$ are in continuous one-to-one correspondence with the set G/H of left cosets of H in G, and we can identify the reduced order parameter space with a coset space: $V = G/H$. G is denoted as unbroken symmetry group, because it characterizes the symmetry of the high temperture phase (in our examples the paramagnetic state) and thus also the symmetry of the free energy density; H is denoted broken symmetry group.

3.4.2 Reduced Order Parameter Spaces for Crystals. From the preceding analysis we can immediately derive the reduced order parameter space for periodic three-dimensional crystals. Since crystals not only possess rotational but also translational symmetry, the unbroken symmetry group G is the full Euclidean group $E(3) = O(3) \wedge T^3$, the broken symmetry group H is the space group S, and V is the coset space $E(3)/S$. An element $g \in E(3)$ consists of a translation $\mathbf{t}$ and a rotation r: $g = \{r, \mathbf{t}\}$. To associate an element of V with a point p of the defected crystal, we have to perform two steps: first a fixed perfect reference crystal has to be selected. Second, at p a copy of the perfect crystal is to be adjusted in such a way, that it coincides locally with the distorted crystal structure. If $g \in E(3)$ is the rigid body operation, which translates and rotates the reference crystal into the adjusted one, then the reduced order parameter at p is $gS \in E(3)/S$.

The question may be raised why we have not taken the affine group Aff(3) as unbroken symmetry group, and for H the crystal symmetry S_A in Aff(3). The elements of Aff(3) can dilate, compress, or shear the crystal lattice. Use of $V_A = \text{Aff}(3)/S_A$ leads to new singularities, like "shear type" defects. However, because a uniform crystal, if sheared, enhances its free energy (in contrast to a rigidly rotated one), the additional singularities have

much higher energy: selecting the unbroken symmetry group amounts to selecting the energy range of the defects.

A word of caution must be added: translations and rotations in the mapping $R^3\backslash D \to E(3)/S$, $\mathbf{x} \mapsto g(\mathbf{x}) = \{r(\mathbf{x}), \mathbf{t}(\mathbf{x})\}$ (where D denotes the defect set) are not independent (Mermin, 1979; Trebin, 1982; Kutka, 1985). Similarly, as a general strain tensor is subjected to compatibility conditions in order to be derivable from a displacement field, also compatiblity relations exist between the fields $\mathbf{r}(\mathbf{x})$ and $\mathbf{t}(\mathbf{x})$ which might restrict the topological defect classification for crystals. No influence of these conditions has been found on the classification of dislocations or disclinations (although the classification of pointlike solitons has been affected, see Section 3.6).

3.4.3 The Symmetry of Quasicrystals. For the topological classification of defects in quasicrystals the notion of unbroken and broken symmetry must be applied to an aperiodic system, which in almost all cases also does not possess a point symmetry. The word symmetry is ill defined without the object, upon which a symmetry operation is acting. In the framework of the projection method, the quasicrystalline system consists of hypercubic lattice L_γ, tiling plane P, and strip S. After our discussion of Section 2.2 it is reasonable to apply the symmetry operations to the lattice L_γ within the active view point, leaving P and S fixed.

Let us consider the case of pentagonal quasicrystals. The translation group of the hypercubic lattice we denote by Z^5. Its rotation group is the hyperoctahedral group $\Omega(5)$. Then, with respect to a *lattice point*, the symmetry group H_L of L_γ is the semidirect product

$$H_L = \Omega(5) \wedge Z^5. \tag{26}$$

However, if we consider all operations with respect to the *origin of* R^5 situated in the tiling plane P, we have to conjugate H_L with a translation $\{1, \gamma\}$ by the shift vector γ:

$$H_L^{\text{conj}} = \{1, \gamma\}^{-1}\Omega(5) \wedge Z^5\{1, \gamma\}. \tag{27}$$

Now we can state, that H_L^{conj} is "a symmetry group of the quasicrystalline pattern", in the sense that a tiling projected from L_γ is identical to one projected from $H_L^{\text{conj}} L_\gamma = L_\gamma$. When conjugating a rotation $\{r, \mathbf{0}\} \in H_L$, we obtain $\{r, -\gamma + r\gamma\}$. Thus, the rotations are accompanied by fractional translations, and H_L^{conj} is in a certain sense nonsymmorphic.

3.4.4 Reduced Order Parameter Space of a Quasicrystal. As in the case of periodic crystals, we identify the reduced order parmeter space of a quasicrystal with a coset space $V = G/H$. What is the unbroken symmetry

group G? It must be equal to or a subgroup of $E(5)$[4] and, for singularities in the low energy range, it must be an invariance group of the free energy of quasicrystals. From Section 2.2 we know, that all patterns of one LI-class are energetically degenerate. Therefore, the elements of G have to be able to rotate or translate the lattice L_γ into all those positions which lead to patterns of *one LI-class* but *arbitrary orientations* in the tiling plane, i.e. they have to fulfill the following conditions:

- The vectors $\mathbf{t}$ in the translations $\{1, \mathbf{t}\} \in G$ are elements of the orthogonal complement of Δ in R^5 (i.e. of the four-dimensional space $R^4 = P \oplus P_\perp$), because the shift vectors $(\gamma + \mathbf{t})$ of the translated lattices $\{1, \mathbf{t}\} L_\gamma = L_{\gamma+\mathbf{t}}$ must have the same projection onto Δ as γ.
- The rotational part G_{rot} of G must be compatible with the restriction posed to the translations. So, G_{rot} is not the group of all possible proper rotations in R^5 (i.e. $SO(5)$), but is reduced to the direct product of all rotations in R^4 with those in Δ, i.e. to $SO(4)_{R^4} \times 1_\Delta$.
- The group $SO(4)_{R^4} \times 1_\Delta$ contains elements, which change the slope of P with respect to the lattice. These rotations must be excluded, because otherwise even the shape of the tiles is altered. Only such rotations of $SO(4)_{R^4}$ are allowed, which belong to the direct product of the in-plane rotations $r_T \in SO(2)_T$ of P with those in $P_\perp$ (i.e. $r_\perp \in SO(2)_\perp$).

Therefore, we arrive at the result:

$$G_{\text{rot}} = SO(2)_T \times SO(2)_\perp \times 1_\Delta \tag{28}$$

and

$$G = G_{\text{rot}} \wedge R^4. \tag{29}$$

The broken symmetry group H is composed of those elements of H_L^{conj}, which are contained in G:

$$H = G \cap H_L^{\text{conj}} = \{1, \gamma\}^{-1} C_5 \wedge T^* \{1, \gamma\}. \tag{30}$$

As in Section (3.2.5), C_5 denotes the group of cyclic permutations of the basis vectors of Z^5. $T^* \in R^4$ is the subgroup of those discrete translations of Z^5 which have no component along Δ. An element $\mathbf{t}^* \in T^*$ has the form

$$\mathbf{t}^* = \sum_{i=1}^{4} n_i \mathbf{a}_i;\ n_i \in Z;\ \mathbf{a}_i = \mathbf{e}_5 - \mathbf{e}_i. \tag{31}$$

The reduced order parameter space for pentagonal quasicrystals follows as:

$$V = (G_{\text{rot}} \wedge R^4)/H. \tag{32}$$

[4] Since we are only investigating classes of loops in V, it suffices to restrict attention to one connected part of V. Therefore, G can be chosen as connected, i.e. it contains only the proper rotations of $O(5)$ yielding the group $SO(5)$.

As in the case of normal crystals, every point in V (i.e. every coset of H in G) corresponds to a perfect system, which arises from the reference system (i.e. the lattice L_γ) by the action of any element of the coset and subsequent projection. In contrast to periodic crystals, two perfect quasiperiodic patterns which belong to different points in V may not be matched by a rigid motion. They are only locally isomorphic and not globally. This is a consequence of the fact that in general the action of an element $g \in G$ on L_γ changes the union of two-faces in the strip S and thus also the tiling itself.

3.4.5 Topological Point Defects in Two-Dimensional Quasicrystals. In two-dimensional ordered structures, topological point defects are classified by the first homotopy group $\pi_1(V)$. If the order parameter space V is known, $\pi_1(V)$ can be determined by standard methods (see, e.g., Trebin, 1982).

Since the group H is discrete, $\pi_1(V)$ is isomorphic to the lift $\bar{H}$ of H into the universal covering group $\bar{G}$ of G (Trebin, 1982):

$$\pi_1(V) = \bar{H} = \{1, \gamma\}^{-1} Z \wedge Z^4 \{1, \gamma\}. \tag{33}$$

An element $r \in Z$ labels a rotation of C_5 by $r \cdot 72°$. An element $(n_1, n_2, n_3, n_4) \in Z^4$ marks a translation of the group T^* by the vector $\mathbf{t}^* = \sum_{i=1}^{4} n_i \mathbf{a}_i$.

Dislocations—If we consider only translational displacements in the pattern, it is sufficient to deal with a reduced order parameter space V_{trans}, which only contains the translational parts of the groups G and H:

$$V_{\text{trans}} = R^4/T^*. \tag{34}$$

This order parameter space already has been investigated by Kléman *et al.* (1986).

The dislocations are classified by the homotopy group $\pi_1(V_{\text{trans}}) = Z^4$ (here the conjugation can be omitted, because $\{1, \gamma\}$ commutes with the elements of Z^4). Each element $(n_1, n_2, n_3, n_4) \in Z^4$ corresponds to the Burgers vector $\mathbf{b} = \mathbf{t}^*$. After encircling the core of the defect, the lattice L_γ has become a lattice $L_{\gamma+\mathbf{b}}$.

In the explicit construction of a dislocation (Section 3.2.2) the shift vector γ was linked to the strip and not to the lattice. The advantage of this choice was the possibility to separate the Volterra process into two steps:

- First, only the strip was bent. Therefore, the tiling remains undistorted and only the mistakes occur (see, e.g., Fig. 7a).
- Second, the four-dimensional lips Σ_1 and Σ_2 of the Volterra process were glued together thus distorting the lattice and the tiling (see, e.g., Fig. 7b).

For the defect classification, however, it proves to be more convenient to distort only the lattice. Of course, both viewpoints are equivalent.

Disclinations—A pure disclination corresponds to the conjugation class of an element $\{1, \gamma\}^{-1}\{r, 0\}\{1, \gamma\}$ of the fundamental group (for the analogous case in a periodic lattice, see Trebin (1982)).

To compute this class, we must conjugate the element $\{1, \gamma\}^{-1}\{r, 0\}\{1, \gamma\}$ by any element $\{1, \gamma\}^{-1}\{s, \mathbf{t}^*\}\{1, \gamma\}$ of the group $\pi_1(V)$:

$$\begin{aligned}\{1, \gamma\}^{-1}\{s, \mathbf{t}^*\}\{r, 0\}\{s, \mathbf{t}^*\}^{-1}\{1, \gamma\} &= \{1, \gamma\}^{-1}\{sr, \mathbf{t}^*\}\{s^{-1}, -s^{-1}\mathbf{t}^*\}\{1, \gamma\} \\ &= \{1, \gamma\}^{-1}\{srs^{-1}, \mathbf{t}^* - srs^{-1}\mathbf{t}^*\}\{1, \gamma\} \\ &= \{1, \gamma\}^{-1}\{r, (1 - r)\mathbf{t}^*\}\{1, \gamma\}. \qquad (35)\end{aligned}$$

The last step is justified because the group C_5 is abelian.

From Eq. (35) we conclude that the conjugation class consists of all elements $\{1, \gamma\}^{-1}\{r, T^*_{\text{sub}}\}\{1, \gamma\}$, where T^*_{sub} denotes a subset of the translational group T^*. For a given r, T^*_{sub} is spanned by the vectors $\{(1 - r)(\mathbf{e}_5 - \mathbf{e}_i)\}$; $i = 1, \ldots, 4$. The vector $\mathbf{t}^*$ in Eq. (35) determines the position of the disclination with respect to the origin of R^5, about which the rotations of the reference lattice are performed.

A disclination at the origin of R^5 (i.e. at the origin of the tiling) is described by the element of $\pi_1(V)$:

$$\{1, \gamma\}^{-1}\{r, 0\}\{1, \gamma\} = \{r, 0\}\{1, -r^{-1}\gamma + \gamma\}. \qquad (36)$$

Equation (36) can be interpreted as follows: before glueing the two lips of the Volterra process together (characterized by $\{r, 0\}$), we have to change the shift vector γ_{start} into $\gamma_{\text{end}} = \{1, r^{-1}\gamma_{\text{start}} - \gamma_{\text{start}}\}\gamma_{\text{start}} = r^{-1}\gamma_{\text{start}}$. This is exactly the modification we had performed in Section 3.2.5.

Disclination dipole—A dislocation is topologically equivalent to a disclination dipole. We demonstrate this statement for a disclination placed at the origin of R^5 and its antidisclination placed at $\mathbf{t} \in Z^5$. For simplicity in the following we omit the conjugation by $\{1, \gamma\}$. The disclination is labelled by

$$\{r, 0\}. \qquad (37)$$

The antidisclination is given by conjugation of $\{r^{-1}, 0\}$ with the vector $\mathbf{t}$:

$$\{1, \mathbf{t}\}\{r^{-1}, 0\}\{1, \mathbf{t}\}^{-1} = \{r^{-1}, (1 - r^{-1})\mathbf{t}\}. \qquad (38)$$

The translational vector in the antidisclination is always contained in the sublattice T^*, hence both defects preserve the original LI-class.

In the topological defect classification the combination of defects is described by the group product (Trebin, 1982). Therefore, for the disclination dipole we get:

$$\{r, 0\}\{r^{-1}, (1 - r^{-1})\mathbf{t}\} = \{1, (r - 1)\mathbf{t}\}. \qquad (39)$$

Equation (39) labels a dislocation with Burgers vector $\mathbf{b} = (r - 1)\mathbf{t}$, which is always an element of T^*.

In Section 3.2.6, a dislocation with Burgers vector $\mathbf{b} = (0, -2, 2, 2, -2)$ was shown (Fig. 15). After a slight adjustment [5] of some tiles near the defect centre, the disclination dipole becomes visible. The two cores (marked by D for disclination and A for antidisclination) are separated by the projection of the vector $\mathbf{t} = (0, -2, 0, 2, 0)$ on the tiling plane.

3.5 *Line Singularities in Icosahedral Quasicrystals*

Icosahedral quasicrystals can be constructed by projection from a six-dimensional hypercubic lattice onto a three-dimensional tiling plane (see, e.g., Katz and Duneau, 1986). Because here in contrast to the two-dimensional case all patterns belong to the same LI-class (Levine and Steinhardt, 1986), for the unbroken symmetry group all translations in six-dimensional space are permitted. The rotational part of G must leave the tiling space invariant; hence

$$G = \{SO(3)_T \times SO(3)_\perp\} \wedge R^6. \tag{40}$$

In the sense of Section 3.4.4 we obtain for the broken symmetry group H of an icosahedral quasicrystal (cp. Eq. 30):

$$\begin{aligned} H &= G \cap \{1, \gamma\}^{-1}\{\Omega(6) \wedge Z^6\}\{1, \gamma\} \\ &= \{1, \gamma\}^{-1}\{A(5) \wedge Z^6\}\{1, \gamma\}. \end{aligned} \tag{41}$$

The full point group $\Omega(6)$ of the hypercubic lattice is reduced to the icosahedral group $A(5)$.

To classify line defects in icosahedral quasicrystals, we have to investigate the fundamental group $\pi_1(V)$, where $V = G/H$ is again the reduced order parameter space (see Section 3.4.4). With the help of standard methods of homotopy theory (Trebin, 1982) we arrive at the result:

$$\pi_1(V) = \{1, \gamma\}^{-1}\{\bar{A}(5) \wedge Z^6\}\{1, \gamma\}. \tag{42}$$

$\bar{A}(5)$ denotes the lift of the icosahedral group into $SU(2)$. The fundamental group classifies dislocation and disclination lines; the Volterra process proceeds as in the two-dimensional case.

[5] Only such adjustments are allowed which lead at the most to the creation of mistakes but leave the LI-class otherwise unchanged.

3.6 A Speculative Remark

The topological theory of defects not only classifies singularities but also topological solitons in ordered media. These are nonsingular mappings $R^d \to V$, which, due to fixed boundary conditions, cannot decay to the uniform ground state. For pointlike topological solitons in particular, which also are denoted configurations, the boundary conditions are such that the reduced order parameter is constant far away from a point. Hence the points at infinity all can be identified, and the mapping can be interpreted as going from the d-dimensional sphere S^d to V, since $S^d = R^d \cup \{\infty\}$. Accordingly, the configurations are labelled by elements of the homotopy group $\pi_d(V)$.

The existence of configurations has been discussed for crystals, and it was found that homotopy theory yields wrong results. Due to compatibility conditions (Gunn and Ma, 1980; Trebin, 1983), configurations are not labelled by elements of $\pi_d(E(d)/H)$, where H denotes the crystal space group, but by the connected components ("islands") of the group of diffeomorphisms $\mathfrak{IC}^d$ of the d-sphere S^d, denoted $\pi_0(\mathfrak{IC}^d)$. For dimension $d = 4$, $\pi_0(\mathfrak{IC}^d)$ is still unknown; for $d = 1, 2, 3, 5$ it is trivial, i.e. no stable configurations exist. For $d = 6$ there are 27 stable configurations, since $\pi_0(\mathfrak{IC}^6) = Z_{28}$, the 28-element cyclic group.

Before the discovery of incommensurate systems the dimensionality of crystals was restricted to 3. With the advent of icosahedral quasicrystals dimension 6—where definitely the first stable configurations are existing—is accessible to observation. If we allow the local patterns to move out of their LI-class, and hence the space of degeneracy to extend to $E(6)/\Omega(6) \wedge Z^6$, three-dimensional cross-sections through six-dimensional configurations may show up as particularly deformed icosahedral quasicrystals.

4 The Motion of Dislocations in Quasicrystals

4.1 Introduction

In Section 3.2.1, some properties of dislocations in periodic crystals were listed. The forces necessary to initiate plastic flow are low in a crystal with dislocations. These defects, which mediate a stepwise shear have a high mobility: to shift a dislocation by one lattice constant a, only a few atoms near the defect core have to jump over distances of the order of a; outside the core the lattice remains essentially unchanged (cp. Fig. 2).

In a quasicrystal, a dislocation is accompanied by mistakes (Section 3.2.3). According to the hydrodynamic theory of Lubensky *et al.* (1986), the mobility of dislocations is strongly reduced due to the fact that their motion is coupled to diffusive modes. It is speculated that, therefore, the plasticity limit is drastically increased.

In this section, we investigate how mistakes are created and how they move in a pentagonal quasiperiodic pattern if the two cores of a dislocation dipole are separated.

4.2 Construction of a Dislocation Dipole

A dislocation dipole consists of two dislocations of opposite Burgers vectors. For the construction of such a dipole in a quasicrystal the two cores are placed at points a and $-a$ on the x-axis of the tiling plane. To bend the strip S_γ properly we introduce two angles θ_1 and θ_2 about each core and interpolate the shift vector γ in the following way:

$$\gamma(\theta_1, \theta_2) = \gamma_{\text{start}} + \frac{\theta_1}{2\pi}\mathbf{b} + \frac{\theta_2}{2\pi}(-\mathbf{b}). \tag{43}$$

The two angles θ_1 and θ_2 are related to the polar angle θ by:

$$\cos\theta_1 = \frac{r\cdot\cos\theta - a}{\sqrt{r^2 + a^2 - 2ra\cos\theta}};\ \cos\theta_2 = \frac{r\cdot\cos\theta + a}{\sqrt{r^2 + a^2 + 2ra\cos\theta}}. \tag{44}$$

The resulting dislocation dipole is depicted in Fig. 17. The lips are not closed and the removed trails are visible (cp. Fig. 7a).

4.3 Creation and Motion of Mistakes

If the two cores of the dislocation dipole are close, the quasicrystal outside the centre remains nearly perfect; only a few mistakes occur. When the cores separate, the two defects become more and more isolated dislocations and the number of mistakes increases. This is demonstrated in Fig. 18 for two different distances.

We study the motion process by looking at the marked mistake. From Fig. 18a to Fig. 18b it has walked along the hatched piece of the trail. On its way several vertices in the trail have jumped to new positions. Outside, the structure is unchanged. Generally, only when mistakes are created (for example the two mistakes marked by 1 in Fig. 18b) or along trails where they move is the structure altered. The rest of the pattern remains untouched.

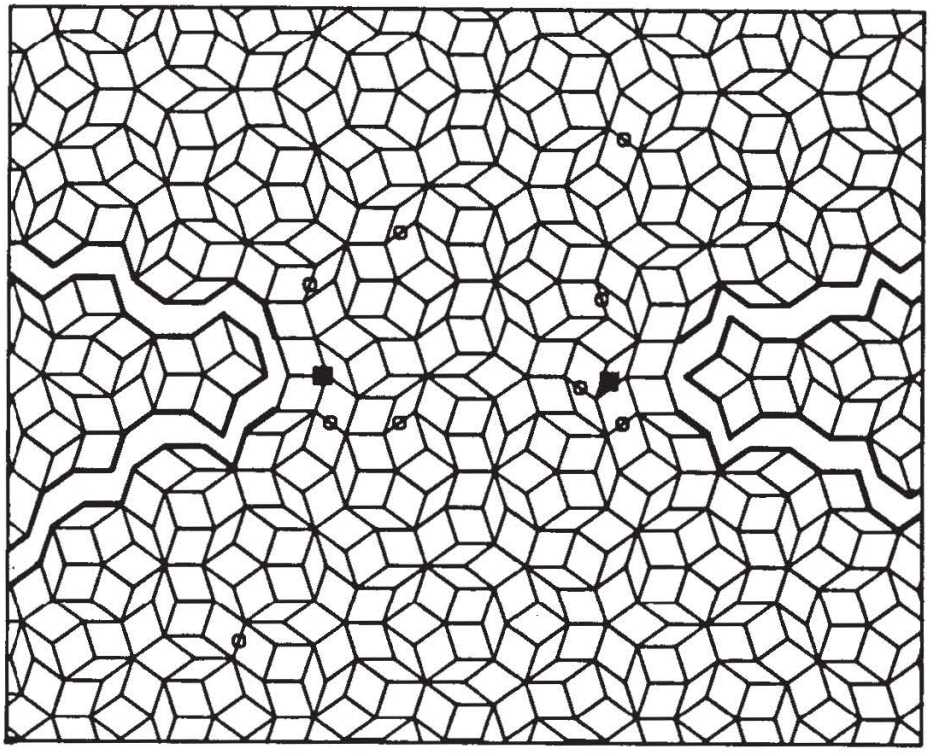

Figure 17. Dislocation dipole in a Penrose pattern of Burgers vector $\mathbf{b} = \pm(0, -1, 0, 0, 1)$. Undistorted state.

The creation and motion process is inquired in detail in Fig. 19, where we have isolated one trail of the defected quasicrystal. In the sequence from Fig. 19a to Fig. 19h the two defect cores (not shown) are separated slowly.

In Fig. 19a no mistake is seen. Fig. 19b demonstrates the creation of a pair of mistakes. It is induced by a jump of the dotted vertex along the arrow of Fig. 19a. The jump can also be interpreted as a flip of the hexagon which contains the dotted vertex.

In the next figures of the sequence, the two mistakes move apart by further jumps of vertices (in Fig. 19d the mistake at the top has left the picture). It is remarkable, that all vertices jump by exactly the same amount.

In summary, the motion of dislocations in quasicrystals is characterized by the following features:

- In contrast to periodic crystals the pattern of a quasicrystal varies outside the core of a moving dislocation. However, the variations are restricted to points where mistakes are created or trails along which they move.
- The creation and motion of mistakes happens by well-defined jumps of vertices. These jumps are the microscopic interpretation of the diffusive modes to which the dislocation motion is coupled in continuum theory (Lubensky *et al.*, 1986).

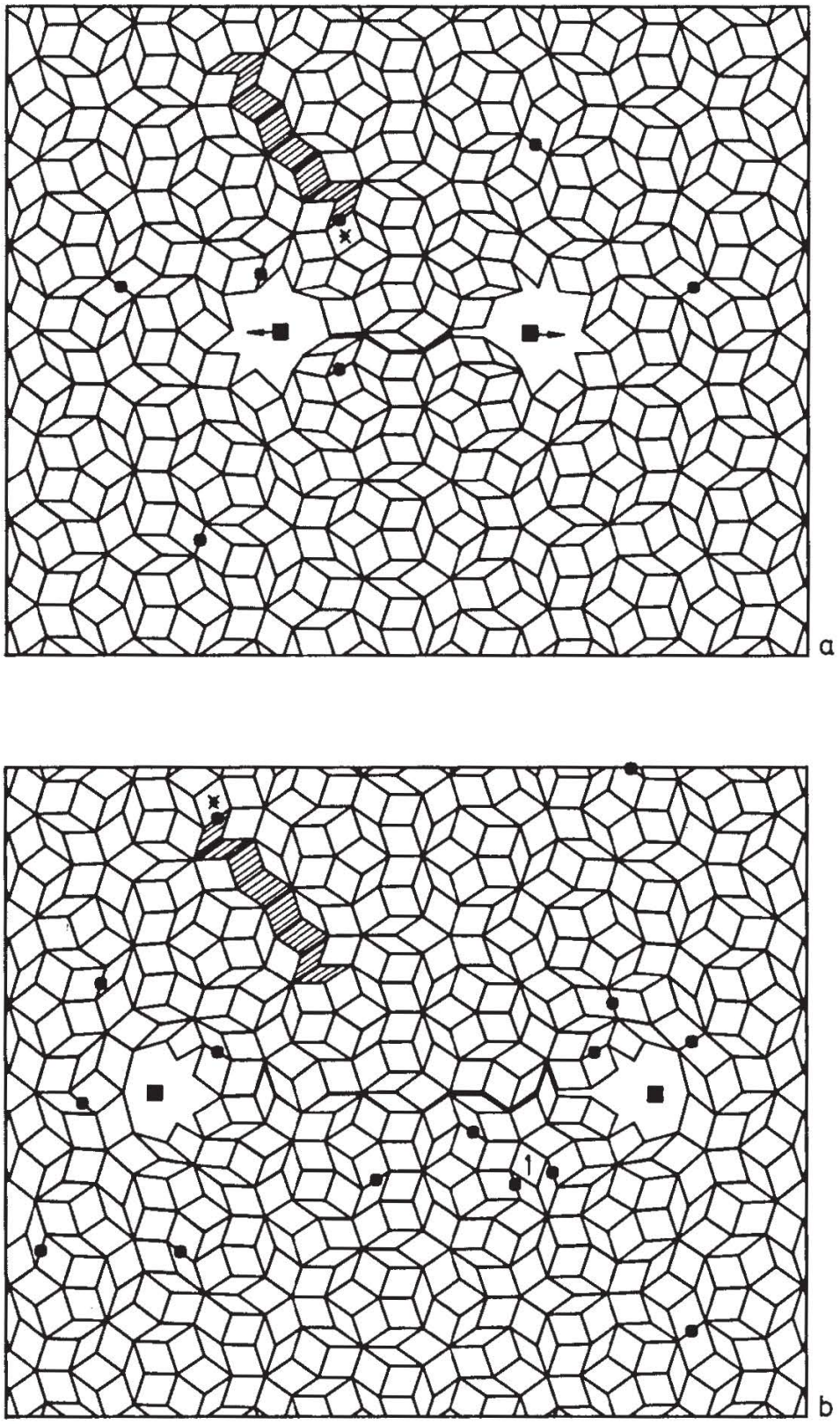

Figure 18. Two dislocation dipoles in a Penrose pattern of different core separation. For details, see text.

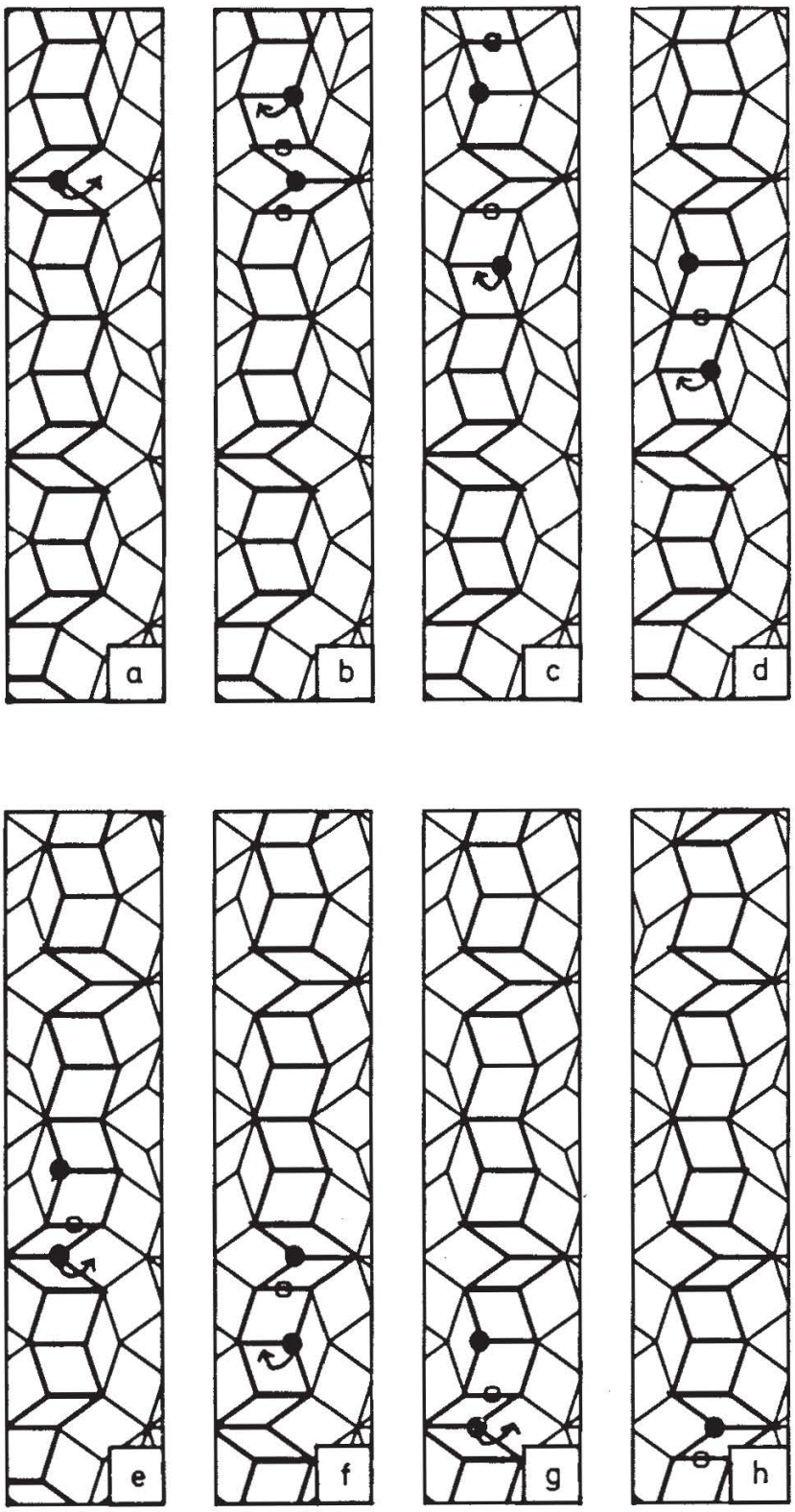

Figure 19. Trail in a quasicrystal, which contains a dislocation dipole. From *a* to *h* the two cores are separated slowly to demonstrate the motion process of a mistake. For details, see text.

5 Conclusion

In the preceding two sections we have constructed topological defects in quasicrystals, which are a generalization of dislocations and disclinations in periodic crystals. In quasicrystals, these singularities always are accompanied by "phason strain", which appears in the form of "mistakes" in the tiling, i.e. by exceptional vertices. At a mistake, the quasicrystal changes from one element of the LI-class to another (see Fig. 9). Thus, mistakes are like kinks of a soliton, regions, where the soliton amplitude moves from one vacuum state to the next. In the language of incommensurate systems, mistakes correspond to discommensurations, which are mismatches in the phase of the modulating incommensurate wave.

At the mistake, the line (or surface in three dimensions), which marks the average position of the trail, performs a discontinuous jump ("jag"). High-resolution transmission electron micrographs along fivefold axes of Al–Mn-quasicrystals display the trails and also reveal mistakes (like in Fig. 1 of Hiraga *et al.* (1985), where a jag is evident in a vertical trail). Also dislocations have been spotted in electron micrographs by counting missing trails along a closed loop (Hiraga and Hirabayashi, 1987).

Urban *et al.* (1985) have reported transitions from the quasicrystalline to the amorphous state of $Al_{86}Mn_{14}$ by electron irradiation. The process was recorded by a series of electron diffraction patterns. These show several of the decagonal stars of sharp diffraction spots gradually developing into rings without change of the radius. The results indicate that the local neighbourhoods of the atoms are preserved while the angular correlations are perturbed. Disclinations as described in this article are candidates for elementary excitations which drive the icosahedral into the amorphous phase. A transition from the glassy to the icosahedral phase was achieved by Poon *et al.* (1985) through annealing, the process, however, was not observed continuously.

We have demonstrated, that a dislocation is equivalent to a disclination dipole. Therefore, in quasicrystals the same mechanisms are present, which in two-dimensional periodic crystals initiate the phase transitions from the crystalline to the hexatic and from the hexatic to the liquid phase, namely stepwise unbinding of disclination quadrupoles (equivalent to dislocation dipoles) into their constituents. According to the kinetics of dislocation and disclination motion, however, it is doubtful whether these processes happen in quasicrystals. The topological defects are surrounded by a cloud of mistakes. They form polaron-type excitations, whose mobility and interaction must be renormalized compared to the case of hexagonal crystals. The mobility is strongly reduced according to the hydrodynamic theories (Lubensky *et al.*, 1986). Because a cloud of mistakes has to be built up in the

successive separation of the disclinations, the binding energy might be so large that the transition temperatures become unreasonably high.

We have seen that the rigid motion characterizing a disclination is composed of a rotation and a fractional translation. Disclinations, therefore, should be more exactly called "dispirations."

Apart from dislocations and disclinations also stacking faults can exist in quasicrystals. They are generated by Volterra cuts just as in the case of dislocations, but without bending of the strip. Twin boundaries, too, can be constructed with the help of many specially arranged dislocations. If we allow local neighbourhoods, which do belong to different LI-classes, then the topological theory predicts many other, highly energetic types of singularities, including sections through six-dimensional pointlike solitons.

References

Bak, P. (1985). Symmetry, stability and elastic properties of icosahedral incommensurate crystals. *Phys. Rev. B* **32**, 5764–5772.

Bohsung, J. and Trebin, H.-R. (1987). Disclinations in quasicrystals. *Phys. Rev. Lett.* **58**, 2277–2280.

de Bruijn, N. G. (1981). Algebraic theory of Penrose's non-periodic tilings of the plane. *Ned. Akad. Weten. Proc. Ser. A* **84**; *Indag. Math. A* **43**, 39–66.

Cheng, M., Ho, J. T., Hui, S. W., Pindak, R. (1987). Electron-diffraction study of free-standing liquid-crystal films. *Phys. Rev. Lett.* **59**, 1112–1115.

Duneau, M. and Katz, A. (1985). Quasiperiodic patterns. *Phys. Rev. Lett.* **54**, 2688–2691.

Friedel, J. (1967). *Dislocations*. Pergamon Press, London.

Friedel, J. (1981). Dislocations and walls in crystals. In *Physics of Defects* (Balian, R., Kléman, M. and Poirier, J.-P., eds.). North Holland Publ. Co., 1–131.

Gähler, F. and Rhyner, J. (1986). Equivalence of the generalized grid and projection methods for the construction of quasiperiodic tilings. *J. Phys. A: Math. Gen.* **19**, 267–277.

Gunn, J. M. F. and Ma, K. B. (1980). On textural defects in crystals. *J. Phys. C* **13**, 963–966.

Halperin, B. I. and Nelson, D. R. (1978). Theory of two-dimensional melting. *Phys. Rev. Lett.* **41**, 121–124.

Harris, W. F. (1970). The dispiration: a distinct new crystal defect of the Weingarten-Volterra type. *Phil. Mag.* **22**, 949–952.

Hiraga, K., Hirabayashi, M., Inoue, A. and Masumoto, T. (1985). Icosahedral quasicrystals of a melt-quenched Al–Mn alloy observed by high-resolution electron microscopy. *Sci. Rep. Inst. Tohokun Univ.* **A32**, 309–314.

Hiraga, K. and Hirabayashi, M. (1987). Dislocations in an Al-Mn-Si icosahedral quasicrystal observed by high-resolution electron microscopy. *Jap. Journ. of Apl. Phys.* **26**, L155–L158.

Jarić, M. V. (1985). Long-range icosahedral orientational order and quasicrystals. *Phys. Rev. Lett.* **55**, 607–610.

Kalugin, P. A., Kitaev, A. and Levitov, L. (1985). $Al_{0.86}Mn_{0.14}$: a six-dimensional crystal. *Pis'ma Zh. Eksp. Teor. Fiz.* **41**, 119–121. *JETP Lett.* **41**, 145–149.

Katz, A. and Duneau, M. (1986). Quasiperiodic patterns and icosahedral symmetry. *J. Phys. (Paris)* **47**, 181–196.

Kléman, M., Gefen, Y. and Pavlovitch, A. (1986). Topological defects in non-Haüyan crystallography: the two-dimensional case. *Europhys. Lett.* **1**, 61–69.

Kramer, P. and Neri, R. (1984). On periodic and non-periodic space-fillings of E^m obtained by projection. *Acta Cryst. A* **40**, 580–587.

Kutka, R. (1985). *Topologische Defektklassifikation mit Nebenbedingungen.* Thesis, University of Regensburg.

Landau, L. D. and Lifshitz, E. M. (1980). *Statistical Physics.* Pergamon Press, London.

Levine, D., Lubensky, T. C., Ostlund, S., Ramaswamy, S., Steinhardt, P. J. and Toner, J. (1985). Elasticity and dislocations in pentagonal and icosahedral quasicrystals. *Phys. Rev. Lett.* **54**, 1520–1523.

Levine, D. and Steinhardt, P. J. (1986). Quasicrystals I: definition and structure. *Phys. Rev. B* **34**, 596–616.

Lu, J. P. and Birman, J. L. (1986). Mistakes in quasilattices. *Phys. Rev. Lett.* **57**, 2701–2705.

Lubensky, T. C., Ramaswamy, S. and Toner, J. (1985). Hydrodynamics of icosahedral quasicrystals. *Phys. Rev. B* **32**, 7444–7452.

Lubensky, T. C., Ramaswamy, S. and Toner, J. (1986). Dislocation motion in quasicrystals and implications for macroscopic properties. *Phys. Rev. B* **33**, 7715–7719.

Mermin, N. D. (1979). The topological theory of defects in ordered media. *Rev. Mod. Phys.* **51**, 591–649.

Nabarro, F. R. (1979). *Dislocations in solids.* North-Holland Publ. Co., Amsterdam.

Nelson, D. R. (1983). Order, frustration, and defects in liquids and glasses. *Phys. Rev. B* **28**, 5515–5535.

Pauling, L. (1987). So-called icosahedral and decagonal quasicrystals are twins of an 820-atom cubic crystal. *Phys. Rev. Lett.* **58**, 365–368.

Penrose, R. (1974). The role of aesthetics in pure and applied mathematical research. *Bull. Inst. Math. Appl.* **10**, 266–271.

Poon, S. J., Drehman, A. J. and Lawless, K. R. (1985). Glassy to icosahedral phase transformation in Pd-U-Si alloys. *Phys. Rev. Lett.* **55**, 2324–2327.

Sachdev, S. and Nelson, R. (1985). Incommensurate icosahedral density waves in rapidly cooled metals. *Phys. Rev. B* **32**, 689–695.

Sadoc, J. F. (1983). Periodic networks of disclination lines: application to metal structures. *J. Phys. Lett. (Paris)* **44**, L707–L715.

Shechtman, P., Gratias, D. and Cahn, J. W. (1984). Metallic phase with long-range orientational order and no translational symmetry. *Phys. Rev. Lett.* **53**, 1951–1954.

Shoemaker, D. P. and Shoemaker, C. B. (1988). Icosahedral coordination in metallic crystals. In *Aperiodicity and Order, Vol. 1* (Jarić, M. V., ed.), Academic Press, 1–57.

Socolar, J. E. S., Lubensky, T. C. and Steinhardt, P. J. (1986). Phonons, phasons, and dislocations in quasicrystals. *Phys. Rev. B* **34**, 3345–3360.

Toulouse, G. and Kléman, M. (1976). Principles of a classification of defects in ordered media. *J. Phys. Lett. (Paris)* **37**, L149–L151.

Träuble, H. and Essmann, U. (1968). Fehler im Flußliniengitter von Supraleitern zweiter Art. *Phys. stat. sol.* **25**, 373–393.

Trebin, H.-R. (1982). The topology of non-uniform media in condensed matter physics. *Adv. Phys.* **31**, 195–254.

Trebin, H.-R. (1983). Configurations in crystals, rod lattices, and lamellar systems. *Phys. Rev. Lett.* **50**, 1381–1384.

Troian, S. and Mermin, N. D. (1985). Mean-field theory of quasicrystalline order. *Phys. Rev. Lett.* **54**, 1524–1527.

Urban, K., Moser, N. and Kronmüller, H. (1985). Phase transitions between the quasicrystalline, crystalline and amorphous phases in Al-14% Mn. *Phys. stat. sol. (a)* **91**, 411–422.

Widom, M. (1988). Short- and long-range icosahedral order in crystals, glass, and quasicrystals. In *Aperiodicity and Order, Vol. 1* (Jarić, M. V., ed.). Academic Press, 59–110.